

<sup>1</sup> Memory for television episodes preserves event content  
<sup>2</sup> while introducing new across-event similarities

<sup>3</sup> Andrew C. Heusser<sup>1,2</sup>, Paxton C. Fitzpatrick<sup>1</sup>, and Jeremy R. Manning<sup>1,\*</sup>

<sup>1</sup>Department of Psychological and Brain Sciences

Dartmouth College, Hanover, NH 03755, USA

<sup>2</sup>Akili Interactive

Boston, MA 02110

\*Corresponding author: jeremy.r.manning@dartmouth.edu

<sup>4</sup> February 5, 2020

<sup>5</sup> **Abstract**

The ways our experiences unfold over time define unique *trajectories* through the relevant representational spaces. Within this geometric framework, one can compare the shape of the trajectory formed by an experience to that defined by our later remembering of that experience. We propose a framework for mapping naturalistic experiences onto geometric spaces that characterize how experiences are segmented into discrete events, and how the contents of event sequences evolve over time. We apply this approach to a naturalistic memory experiment which had participants view and recount a television episode. The content of participants' recounts of events from the original episode closely matched the original episode's content. However, the similarity patterns *across* events was much different in the original episode as compared with participants' recounts. We also identified a network of brain structures that are sensitive to the "shapes" of ongoing experiences, and an overlapping network that is sensitive (at the time of encoding) to how people later remembered those experiences in relation to other experiences.

18 In this way, modeling the content of richly structured experiences can reveal how (geometrically  
19 and conceptually) those experiences are segmented into events and integrated into our memories  
20 of other experiences.

21 **Introduction**

22 What does it mean to *remember* something? In traditional episodic memory experiments (e.g.,  
23 list-learning or trial-based experiments; Murdock, 1962; Kahana, 1996), remembering is often cast  
24 as a discrete and binary operation: each studied item may be separated from all others, and la-  
beled as having been recalled or forgotten. More nuanced studies might incorporate self-reported  
25 confidence measures as a proxy for memory strength, or ask participants to discriminate between  
26 “recollecting” the (contextual) details of an experience or having a general feeling of “familiarity”  
27 (Yonelinas, 2002). Using well-controlled, trial-based experimental designs, the field has amassed  
28 a wealth of valuable information regarding human episodic memory. However, there are funda-  
29 mental properties of the external world and our memories that trial-based experiments are not well  
30 suited to capture (for review also see Koriat and Goldsmith, 1994; Huk et al., 2018). First, our expe-  
31 riences and memories are continuous, rather than discrete—removing a (naturalistic) event from  
32 the context in which it occurs can substantially change its meaning. Second, the specific language  
33 used to describe an experience has little bearing on whether the experience should be considered to  
34 have been “remembered.” Asking whether the rememberer has precisely reproduced a specific set  
35 of words to describe a given experience is nearly orthogonal to whether they were actually able to  
36 remember it. In classic (e.g., list-learning) memory studies, by contrast, the number or proportion  
37 of precise recalls is often a primary metric for assessing the quality of participants’ memories.  
38 Third, one might remember the *essence* (or a general summary) of an experience but forget (or  
39 neglect to recount) particular details. Capturing the essence of what happened is typically the  
40 main “point” of recounting a memory to a listener, while the addition of highly specific details  
41 may add comparatively little to successful conveyance of an experience.  
42

43 How might one go about formally characterizing the “essence” of an experience, or whether

44 it has been recovered by the rememberer? Any given moment of an experience derives meaning  
45 from surrounding moments, as well as from longer-range temporal associations (Lerner et al.,  
46 2011; Manning, 2019). Therefore, the timecourse describing how an event unfolds is fundamental  
47 to its overall meaning. Further, this hierarchy formed by our subjective experiences at different  
48 timescales defines a *context* for each new moment (e.g., Howard and Kahana, 2002; Howard et al.,  
49 2014), and plays an important role in how we interpret that moment and remember it later (for  
50 review see Manning et al., 2015). Our memory systems can leverage these associations to form  
51 predictions that help guide our behaviors (Ranganath and Ritchey, 2012). For example, as we  
52 navigate the world, the features of our subjective experiences tend to change gradually (e.g., the  
53 room or situation we are in at any given moment is strongly temporally autocorrelated), allowing  
54 us to form stable estimates of our current situation and behave accordingly (Zacks et al., 2007;  
55 Zwaan and Radvansky, 1998).

56 Occasionally, this gradual “drift” of our ongoing experience is punctuated by sudden changes,  
57 or “shifts” (e.g., when we walk through a doorway; Radvansky and Zacks, 2017). Prior research  
58 suggests that these sharp transitions (termed *event boundaries*) help to discretize our experiences  
59 (and their mental representations) into *events* (Radvansky and Zacks, 2017; Brunec et al., 2018;  
60 Heusser et al., 2018a; Clewett and Davachi, 2017; Ezzyat and Davachi, 2011; DuBrow and Davachi,  
61 2013). The interplay between the stable (within-event) and transient (across-event) temporal  
62 dynamics of an experience also provides a potential framework for transforming experiences into  
63 memories that distill those experiences down to their essence. For example, prior work has shown  
64 that event boundaries can influence how we learn sequences of items (Heusser et al., 2018a; DuBrow  
65 and Davachi, 2013), navigate (Brunec et al., 2018), and remember and understand narratives (Zwaan  
66 and Radvansky, 1998; Ezzyat and Davachi, 2011). Prior research has implicated the hippocampus  
67 and the medial prefrontal cortex as playing a critical role in transforming experiences into structured  
68 and consolidated memories (Tompry and Davachi, 2017).

69 Here we sought to examine how the temporal dynamics of a “naturalistic” experience were  
70 later reflected in participants’ memories. We analyzed an open dataset that comprised behavioral  
71 and functional Magnetic Resonance Imaging (fMRI) data collected as participants viewed and then

72 verbally recounted an episode of the BBC television series *Sherlock* (Chen et al., 2017). We developed  
73 a computational framework for characterizing the temporal dynamics of the moment-by-moment  
74 content of the episode, and of participants' verbal recalls. Specifically, we use topic modeling (Blei  
75 et al., 2003) to characterize the thematic conceptual (semantic) content present in each moment of  
76 the episode and recalls, and Hidden Markov Models (Rabiner, 1989; Baldassano et al., 2017) to  
77 discretize this evolving semantic content into events. In this way, we cast naturalistic experiences  
78 (and recalls of those experiences) as geometric *trajectories* that describe how the experiences evolve  
79 over time. Under this framework, successful remembering entails verbally "traversing" the content  
80 trajectory of the episode, thereby reproducing the shape (or essence) of the original experience.  
81 Comparing the shapes of the topic trajectories of the episode and of participants' retellings of  
82 the episode then reveals which aspects of the episode were preserved (or lost) in the translation  
83 into memory. We further introduce two novel metrics for assessing memory quality: the *precision*  
84 with which a participant recounts each event and 2) the *distinctiveness* of each recall event (relative  
85 to other recalled events). We examine how these metrics relate to participants' overall memory  
86 performance, and discuss the ways in which they improve upon classic "proportion-recalled"  
87 measures for analyzing naturalistic memory. Last, we utilize our framework to identify networks  
88 of brain structures whose responses (as participants watched the episode) reflected the temporal  
89 dynamics of the episode, and how participants would later recount it.

## 90 Results

91 To characterize the "essence" of the *Sherlock* episode and participants' subsequent recounts of  
92 its unfolding, we used a topic model (Blei et al., 2003) to discover the latent themes in the episode's  
93 dynamic content. Topic models take as inputs a vocabulary of words to consider and a collection  
94 of text documents, and return two output matrices. The first of these is a *topics matrix* whose rows  
95 are topics (latent themes) and whose columns correspond to words in the vocabulary. The entries  
96 of the topics matrix define how each word in the vocabulary is weighted by each discovered topic.  
97 For example, a detective-themed topic might weight heavily on words like "crime," and "search."

98 The second output is a *topic proportions matrix*, with one row per document and one column per  
99 topic. The topic proportions matrix describes what mixture of discovered topics is reflected in each  
100 document.

101 Chen et al. (2017) collected hand-annotated information about each of 1000 (manually identified)  
102 time segments spanning the roughly 50 minute video used in their experiment. This information  
103 included: a brief narrative description of what was happening, the location where the scene  
104 took place, the names of any characters on the screen, and other similar details (for a full list of  
105 annotated features, see *Methods*). We took from these annotations the union of all unique words  
106 (excluding stop words, such as “and,” “or,” “but,” etc.) across all features and scenes as the  
107 “vocabulary” for the topic model. We then concatenated the sets of words across all features  
108 contained in overlapping, sliding windows of (up to) 50 scenes, and treated each window as a  
109 single “document” for the purpose of fitting the topic model. Next, we fit a topic model with (up  
110 to)  $K = 100$  topics to this collection of documents. We found that 32 unique topics (with non-zero  
111 weights) were sufficient to describe the time-varying content of the video (see *Methods*; Figs. 1, S2).  
112 Note that our approach is similar in some respects to Dynamic Topic Models (Blei and Lafferty,  
113 2006) in that we sought to characterize how the thematic content of the episode evolved over  
114 time. However, whereas Dynamic Topic Models are designed to characterize how the properties  
115 of *collections* of documents change over time, our sliding window approach allows us to examine  
116 the topic dynamics within a single document (or video). Specifically, our approach yielded (via the  
117 topic proportions matrix) a single *topic vector* for each sliding window of annotations transformed  
118 by the topic model. We then stretched the resulting windows-by-topics matrix to match the time  
119 series of the 1976 fMRI volumes collected as participants viewed the episode.

120 The 32 topics we found were heavily character-focused (i.e., the top-weighted word in each  
121 topic was nearly always a character) and could be roughly divided into themes centered around  
122 Sherlock Holmes (the titular character), John Watson (Sherlock’s close confidant and assistant),  
123 supporting characters (e.g., Inspector Lestrade, Sergeant Donovan, or Sherlock’s brother Mycroft),  
124 or the interactions between various pairs of these characters (see Fig. S2). Several of the identified  
125 topics were highly similar, which we hypothesized might allow us to distinguish between subtle

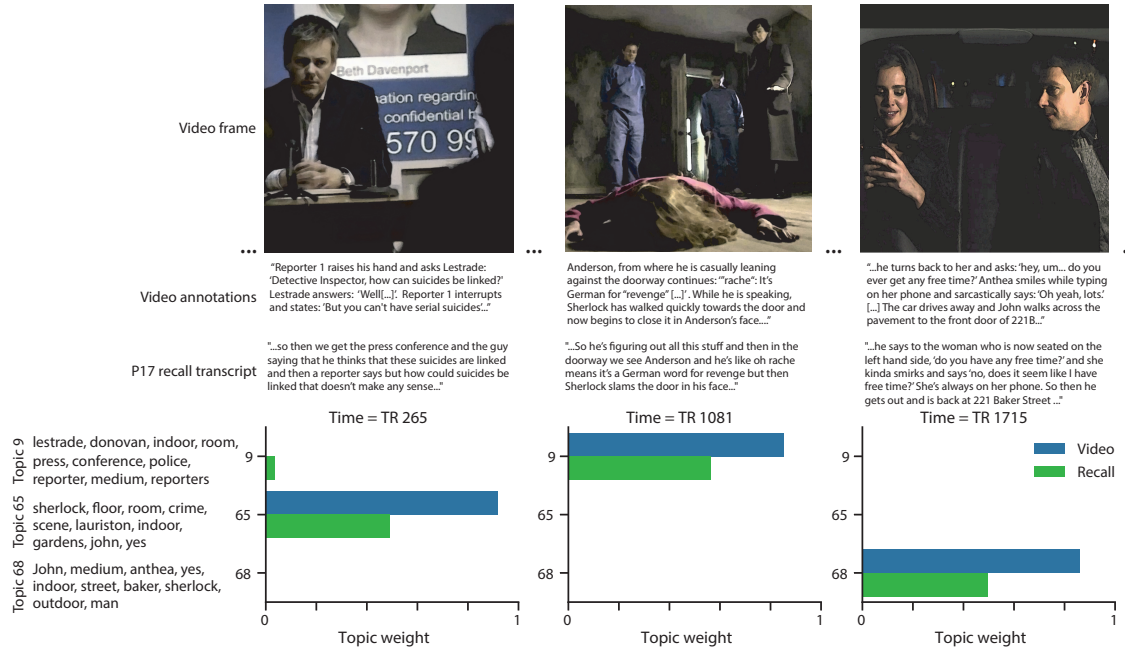


**Figure 1: Methods overview.** We used hand-annotated descriptions of each moment of video to fit a topic model. Three example video frames and their associated descriptions are displayed (top two rows). Participants later recalled the video (in the third row, we show example recalls of the same three scenes from participant 13). We used the topic model (fit to the annotations) to estimate topic vectors for each moment of video and each sentence the participants recalled. Example topic vectors are displayed in the bottom row (blue: video annotations; green: example participant’s recalls). Three topic dimensions are shown (the highest-weighted topics for each of the three example scenes, respectively). We also show the 10 highest-weighted words for each topic. Figure S2 provides a full list of the top 10 words from each of the discovered topics.

126 narrative differences if the distinctions between those overlapping topics were meaningful. The  
127 topic vectors for each timepoint were *sparse*, in that only a small number (usually one or two) of  
128 topics tended to be “active” in any given timepoint (Fig. 2A). Further, the dynamics of the topic  
129 activations appeared to exhibit *persistence* (i.e., given that a topic was active in one timepoint, it was  
130 likely to be active in the following timepoint) along with *occasional rapid changes* (i.e., occasionally  
131 topics would appear to spring into or out of existence). These two properties of the topic dynamics  
132 may be seen in the block diagonal structure of the timepoint-by-timepoint correlation matrix  
133 (Fig. 2B) and reflect the gradual drift and sudden shifts fundamental to the temporal dynamics of  
134 real-world experiences. Given this observation, we adapted an approach devised by Baldassano  
135 et al. (2017), and used a Hidden Markov Model (HMM) to identify the *event boundaries* where the  
136 topic activations changed rapidly (i.e., at the boundaries of the blocks in the correlation matrix;  
137 event boundaries identified by the HMM are outlined in yellow in Fig. 2B). Part of our model fitting  
138 procedure required selecting an appropriate number of “events” into which the topic trajectory  
139 should be segmented. To accomplish this, we used an optimization procedure that maximized the  
140 difference between the topic weights for timepoints within an event and across multiple events  
141 (see *Methods* for additional details). We then created a stable “summary” of the content within  
142 each video event by averaging the topic vectors across timepoints each event spanned (Fig. 2C).

143 Given that the time-varying content of the video could be segmented cleanly into discrete  
144 events, we wondered whether participants’ recalls of the video also displayed a similar structure.  
145 We applied the same topic model (already trained on the video annotations) to each participant’s  
146 recalls. Analogous to how we parsed the time-varying content of the video, to obtain similar esti-  
147 mates for each participant’s recall, we treated each overlapping “window” of (up to 10) sentences  
148 from their transcript as a “document,” and computed the most probable mix of topics reflected in  
149 each timepoint’s sentences. This yielded, for each participant, a number-of-windows by number-  
150 of-topics topic proportions matrix that characterized how the topics identified in the original video  
151 were reflected in the participant’s recalls. Note that an important feature of our approach is that it  
152 allows us to compare participants’ recalls to events from the original video, despite different par-  
153 ticipants using widely varying language to describe the same event, and that those descriptions



**Figure 2: Modelling naturalistic stimuli and recalls.** All panels: darker colors indicate greater values; range: [0, 1]. **A.** Topic vectors ( $K = 100$ ) for each of the 1976 video timepoints. **B.** Timepoint-by-timepoint correlation matrix of the topic vectors displayed in Panel A. Event boundaries discovered by the HMM are denoted in yellow (30 events detected). **C.** Average topic vectors for each of the 30 video events. **D.** Topic vectors for each of 265 sliding windows of sentences spoken by an example participant while recalling the video. **E.** Timepoint-by-timepoint correlation matrix of the topic vectors displayed in Panel D. Event boundaries detected by the HMM are denoted in yellow (22 events detected). For similar plots for all participants see Figure S4. **F.** Average topic vectors for each of the 22 recalled events from the example participant. **G.** Correlations between the topic vectors for every pair of video events (Panel C) and recalled events (from the example participant; Panel F). For similar plots for all participants, see Figure S5. **H.** Average correlations between each pair of video events and recalled events (across all 17 participants). To create the figure, each recalled event was assigned to the video event with the most correlated topic vector (yellow boxes in panels G and H). The heat maps in each panel were created using Seaborn (Waskom et al., 2016).

<sup>154</sup> may not match the original annotations. This is a substantial benefit of projecting the video and  
<sup>155</sup> recalls into a shared “topic” space. An example topic proportions matrix from one participant’s  
<sup>156</sup> recalls is shown in Figure 2D.

<sup>157</sup> Although the example participant’s recall topic proportions matrix has some visual similarity to  
<sup>158</sup> the video topic proportions matrix, the time-varying topic proportions for the example participant’s  
<sup>159</sup> recalls are not as sparse as those for the video (compare Figs. 2A and D). Similarly, although there do  
<sup>160</sup> appear to be periods of stability in the recall topic dynamics (i.e., most topics are active or inactive  
<sup>161</sup> over contiguous blocks of time), the individual topics’ overall timecourses are not as cleanly  
<sup>162</sup> delineated as the video topics’. To examine these patterns in detail, we computed the timepoint-  
<sup>163</sup> by-timepoint correlation matrix for the example participant’s recall topic trajectory (Fig. 2E). As  
<sup>164</sup> in the video correlation matrix (Fig. 2B), the example participant’s recall correlation matrix has a  
<sup>165</sup> strong block diagonal structure, indicating that their recalls are discretized into separated events.  
<sup>166</sup> As for the video correlation matrix, we can use an HMM, along with the aforementioned number-  
<sup>167</sup> of-events optimization procedure (also see *Methods*) to determine how many events are reflected  
<sup>168</sup> in the participant’s recalls and where specifically the event boundaries fall (outlined in yellow).  
<sup>169</sup> We carried out a similar analysis on all 17 participants’ recall topic proportions matrices (Fig. S4).

<sup>170</sup> Two clear patterns emerged from this set of analyses. First, although every individual partic-  
<sup>171</sup> ipant’s recalls could be segmented into discrete events (i.e., every individual participant’s recall  
<sup>172</sup> correlation matrix exhibited clear block diagonal structure; Fig. S4), each participant appeared to  
<sup>173</sup> have a unique *recall resolution*, reflected in the sizes of those blocks. While, some participants’ recall  
<sup>174</sup> topic proportions segmented into just a few events (e.g., Participants P4, P5, and P7), others’ seg-  
<sup>175</sup> mented into many shorter duration events (e.g., Participants P12, P13, and P17). This suggests that  
<sup>176</sup> different participants may be recalling the video with different levels of detail— e.g., some might  
<sup>177</sup> touch on just the major plot points, whereas others might attempt to recall every minor scene or ac-  
<sup>178</sup> tion. The second clear pattern present in every individual participant’s recall correlation matrix is  
<sup>179</sup> that, unlike in the video correlation matrix, there are substantial off-diagonal correlations. Whereas  
<sup>180</sup> each event in the original video was (largely) separable from the others (Fig. 2B), in transforming  
<sup>181</sup> those separable events into memory, participants appear to be integrating across multiple events,

182 blending elements of previously recalled and not-yet-recalled content into each newly recalled  
183 event (Figs. 2D, S4; also see Manning et al., 2011; Howard et al., 2012).

184 The above results indicate that both the structure of the original video and participants' recalls  
185 of the video exhibit event boundaries that can be identified automatically by characterizing the  
186 dynamic content using a shared topic model and segmenting the content into events via HMMs.  
187 Next, we asked whether some correspondence might be made between the specific content of the  
188 events the participants experienced in the video, and the events they later recalled. One approach  
189 to linking the experienced (video) and recalled events is to label each recalled event as matching  
190 the video event with the most similar (i.e., most highly correlated) topic vector (Figs. 2G, S5). This  
191 yields a sequence of "presented" events from the original video, and a (potentially differently  
192 ordered) sequence of "recalled" events for each participant. Analogous to classic list-learning  
193 studies, we can then examine participants' recall sequences by asking which events they tended  
194 to recall first (probability of first recall; Fig. 3A; Atkinson and Shiffrin, 1968; Postman and Phillips,  
195 1965; Welch and Burnett, 1924); how participants most often transition between recalls of the  
196 events as a function of the temporal distance between them (lag-conditional response probability;  
197 Fig. 3B; Kahana, 1996); and which events they were likely to remember overall (serial position  
198 recall analyses; Fig. 3C; Murdock, 1962). Interestingly, for two of these analyses (probability of first  
199 recall and lag-conditional response probability curves) we observe patterns comparable to classic  
200 effects from the list-learning literature: namely, a higher probability of initiating recall with the  
201 first event in the sequence (Fig. 3A) and a higher probability of transitioning to neighboring events  
202 with an asymmetric forward bias (Fig. 3C). In contrast, we do not observe a pattern comparable to  
203 the serial position effect (Fig. 3C), but rather we see higher memory for specific events distributed  
204 somewhat evenly throughout the video.

205 We can also apply two list-learning-native analyses that describe how participants group items  
206 in their recall sequences: temporal clustering and semantic clustering (Polyn et al., 2009, see  
207 *Methods* for details). Temporal clustering refers to the extent to which participants group their  
208 recall responses according to encoding position. Overall, we found that sequentially viewed video  
209 events were clustered heavily in participants' recall event sequences (mean: 0.767, SEM: 0.029),

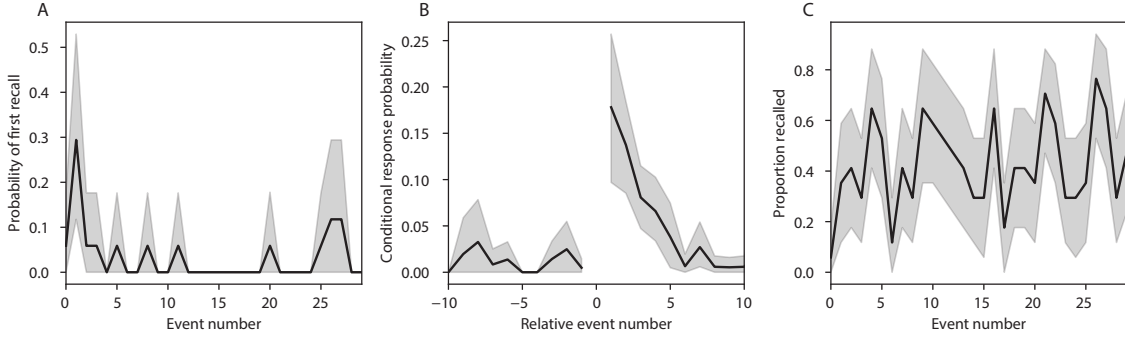


**Figure 3: Naturalistic extensions of classic list-learning memory analyses.** **A.** The probability of first recall as a function of the serial position of the event in the video. **B.** The probability of recalling each event, conditioned on having most recently recalled the event *lag* events away in the video. **C.** The proportion of participants who recalled each event, as a function of the serial position of the events in the video. All panels: error bars denote bootstrap-estimated standard error of the mean.

and that participants with higher temporal clustering scores tended to perform better according to both Chen et al. (2017)'s hand-annotated memory scores (Pearson's  $r(15) = 0.62$ ,  $p = 0.008$ ) and our model's estimate (Pearson's  $r(15) = 0.54$ ,  $p = 0.024$ ). Semantic clustering measures the extent to which participants cluster their recall responses according to semantic similarity. We found that participants tended to recall semantically similar video events together (mean: 0.787, SEM: 0.018), and that semantic clustering score was also related to both hand-annotated (Pearson's  $r(15) = 0.65$ ,  $p = 0.004$ ) and model-derived (Pearson's  $r(15) = 0.63$ ,  $p = 0.007$ ) memory performance.

Statistical models of memory studies often treat recall success as binary (i.e., an item either was or was not recalled), or occasionally categorical (e.g., to distinguish familiarity from recollection; Yonelinas et al., 2002). Such approaches are tenable in classical list-learning or recognition memory paradigms, as the presented stimuli tend to be very simple (e.g., a sequence of individual words or items). However, the feature-rich content of a naturalistic experiences may later be described with many, highly variable levels of success. Our framework produces a content-based model of individual stimulus and recall events by projecting the dynamic content of the video and participants' recalls into a shared topic space. This allows for direct, quantitative comparison between all stimulus and recall events, as well as between the recall events themselves. Leveraging

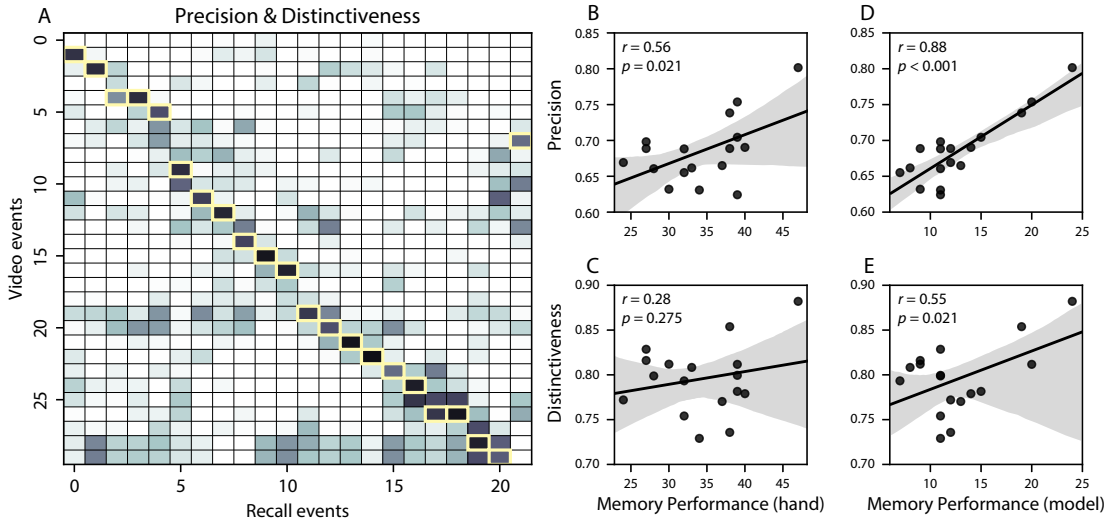


**Figure 4: Novel content-based metrics of naturalistic memory: precision and distinctiveness.** A. The video-recall correlation matrix for a representative participant (17). The yellow boxes highlight the maximum correlation in each column. The example participant's overall precision score was computed as the average across correlation values in the yellow boxes. Their distinctiveness score was computed as the the average (over recall events) of 1 minus the average correlation between each recall event and all other recall events that do not display a box in the same row. B. The (Pearson's) correlation between precision and hand-annotated memory performance. C. The correlation between distinctiveness and hand-annotated memory performance. D. The correlation between precision and the number of video events successfully recalled, as determined by our model. E. The correlation between distinctiveness and the number of video events successfully recalled, as determined by our model.

these content-based models of the stimulus/recall events, we developed two novel, *continuous* metrics for analyzing naturalistic memory: *precision* and *distinctiveness*. We define precision as the “completeness” of recall, or how fully the presented content was recapitulated in memory. Under our framework, we quantify this for a given recall event as the correlation between the topic proportions of the recall event and the maximally correlated video event (Fig. 4). A second novel metric we introduce here is *distinctiveness*, which we define as the “specificity” of recall, or how unique the description of a given section of content was, compared to descriptions for other sections of content. We quantify this for each recall event as 1 minus the average correlation between the given recall event and all other recall events not matched to the same video event. In addition to individual events, one may also use these metrics to describe each participant’s

237 overall performance (i.e., by averaging across a participant’s event-wise precision or distinctiveness  
238 scores). Participants whose recall events are more veridical descriptions of what happened in the  
239 video event will presumably have higher precision scores. We find that, across participants,  
240 a higher precision score is correlated to both hand-annotated memory performance (Pearson’s  
241  $r(15) = 0.56, p = 0.021$ ) and the number of video events successfully remembered, as determined  
242 by our model (Pearson’s  $r(15) = 0.88, p < 0.001$ ). We also hypothesized that participants who  
243 recounted events in a more distinctive way would display better overall memory. We find that  
244 this distinctiveness score is related to our model’s estimated number of recalled events (Pearson’s  
245  $r(15) = 0.55, p = 0.021$ ), and while we do not find distinctiveness to be related to hand-annotated  
246 memory performance (Pearson’s  $r(15) = 0.28, p = 0.275$ ), this is not entirely surprising given how  
247 the hand-annotated memory scores were computed (see *Methods*).

248 Further intuition for the behaviors captured by these two metrics may be gained by directly  
249 examining the content of the video and recalls our framework models. In Figure 5, we contrast  
250 recalls for the same video event (event 22) from two participants: one with a high precision score  
251 (P17), the other with a low precision score (P6). From the HMM-identified event boundaries,  
252 we recovered the set of annotations describing the content of an example video event (Fig. 5B),  
253 and divided them into different color-coded sections for each action or feature described. We  
254 then similarly recovered the set of sentences comprising the corresponding recall event for each  
255 of the two example participants. Because the recall sliding windows overlap heavily, and each  
256 recall event spans multiple recall timepoints (i.e., windows), we have stripped any sentences from  
257 the beginning and end that describe earlier or later video events for the sake of readability. In  
258 other words, Fig. 5C shows a subset of the full recall event text, comprising sentences between  
259 the first and last descriptions of content from the example video event. We then colored all words  
260 describing actions and features coded in panel B by their corresponding color. Visual comparison  
261 of the transcripts reveals that the most precise participant’s recall both captures more of the video  
262 event’s content, and does so with far more detail.

263 Figure 6 similarly contrasts two example participants’ recalls for a common video event (event  
264 19) to illustrate the tangible differences between high and low distinctiveness scores. Here, we

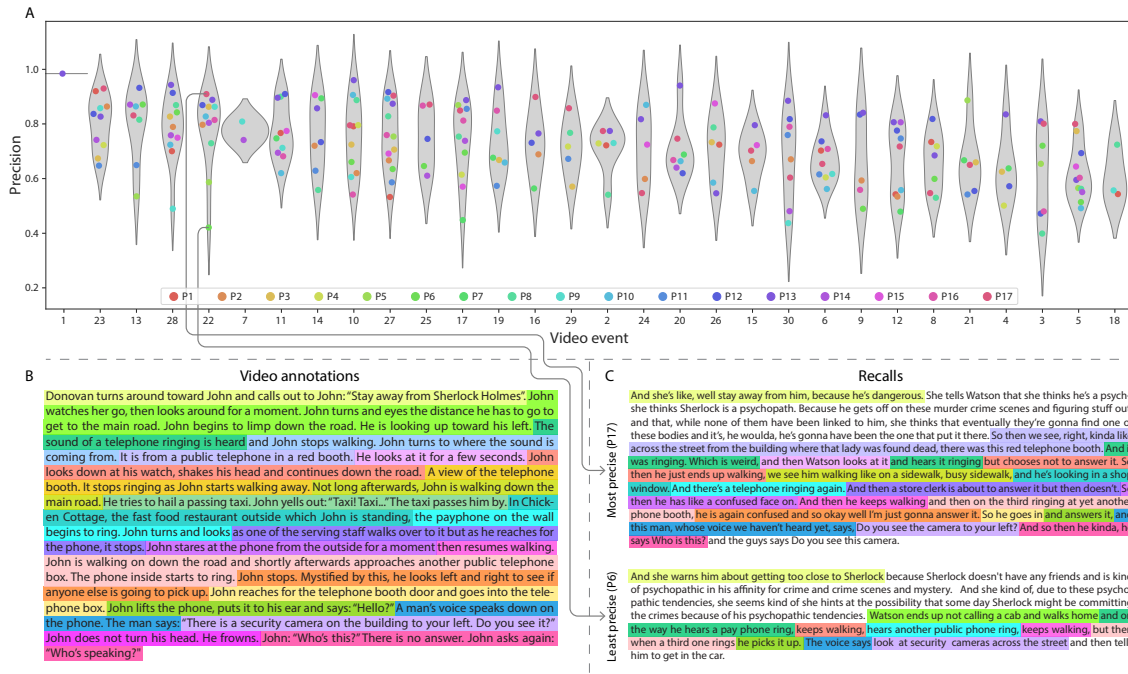


**Figure 5: Precision metric reflects completeness of recall.** **A.** Recall precision by video event. Grey violin plots display kernel density estimates for the distribution of recall precision scores for a single video event. Colored dots within each violin plot represent individual participants' recall precision for the given event. Video events are ordered along the *x*-axis by the average precision with which they were remembered. **B.** The set of "Narrative Details" video annotations (generated by Chen et al., 2017) for scenes comprising an example video event (22) identified by the HMM. Each action or feature is highlighted in a different color. **C.** A subset of the sentences comprising the most precise (P17) and least precise (P6) participants' recalls of video event 22. Descriptions of specific actions or features reflecting those highlighted in panel B are highlighted in the corresponding color.

265 have extracted the full set of sentences comprising the most distinctive recall event (P13) and least  
 266 distinctive recall event (P11) recall event matched to the example video event (Fig. 6C). We also  
 267 extracted the annotations for the example video event, as well as those from each other video  
 268 event whose content the example participants' single recall events described (Fig. 6B). We then  
 269 shaded the annotation text for each video event with a different color, and shaded each word of  
 270 the example participants' recall text by the color of the video event it describes. The majority of  
 271 the most distinctive recall event text describes video event 19's content, with the first five and last  
 272 one sentence describing the video events immediately preceding and succeeding the current one,  
 273 respectively. Meanwhile, the least precise participant's recall for video event 19 blends the content

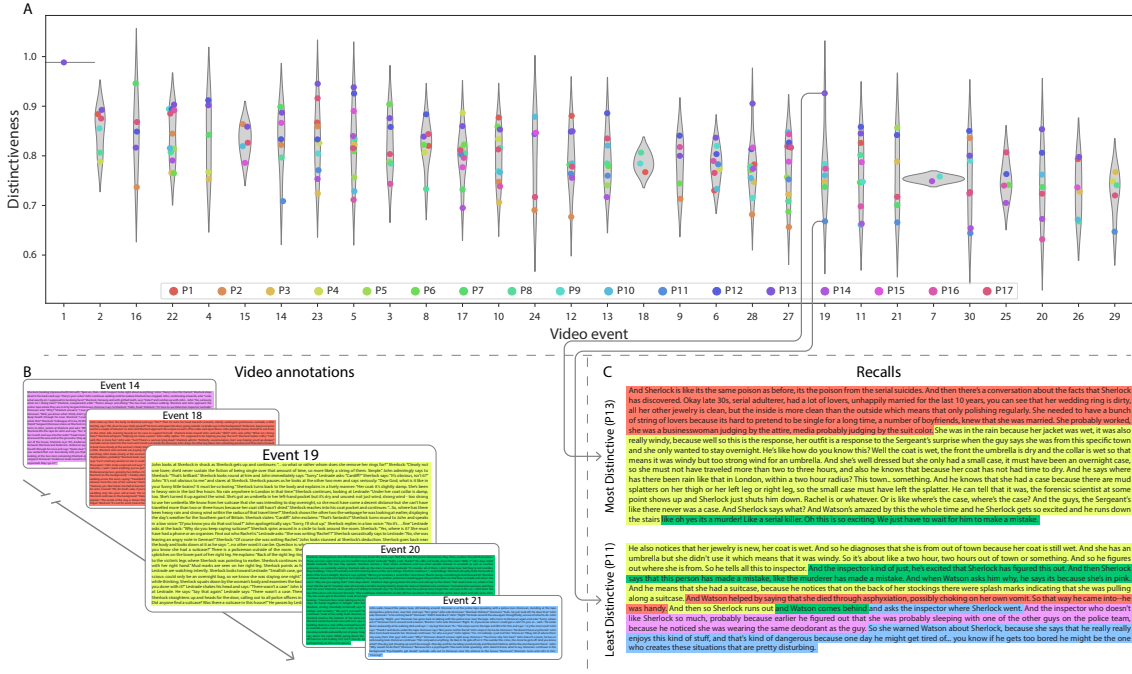


**Figure 6: Distinctiveness metric reflects specificity of recall.** A. Recall distinctiveness by video event. Kernel density estimates for each video event’s distribution of recall distinctiveness scores, analogous to Fig. 5A. B. The sets of “Narrative Details” video annotations (generated by Chen et al., 2017) for scenes comprising video events described by the example participants in panel C. Each event’s text is highlighted in a different color. C. The sentences comprising the most distinctive (P13) and least distinctive (P11) participants’ recalls of video event 19. Sections of recall describing each video event in panel B are highlighted with the corresponding color.

from five separate video events, does not transition between them in order, and often combines descriptions of two video events' content in the same sentence

The prior analyses leverage the correspondence between the 100-dimensional topic proportion matrices for the video and participants' recalls to characterize recall. However, it is difficult to gain deep insights into the content of (or relationships between) experiences and memories solely by examining these topic proportions (e.g., Figs. 2A, D) or the corresponding correlation matrices (Figs. 2B, E, S4). And while we can directly examine the original text underlying these topic vectors (e.g., Figs. 5, 6) to show how relationships between them reflect real-world behavior, this comparison becomes prohibitively cumbersome at larger timescales. To visualize the time-varying high-dimensional content in a more intuitive way (Heusser et al., 2018b) we projected the topic

284 proportions matrices onto a two-dimensional space using Uniform Manifold Approximation and  
285 Projection (UMAP; McInnes et al., 2018). In this lower-dimensional space, each point represents a  
286 single video or recall event, and the distances between the points reflect the distances between the  
287 events' associated topic vectors (Fig. 7). In other words, events that are nearer to each other in this  
288 space are more semantically similar, and those that are farther apart are less so.

289 Visual inspection of the video and recall topic trajectories reveals a striking pattern. First,  
290 the topic trajectory of the video (which reflects its dynamic content; Fig. 7A) is captured nearly  
291 perfectly by the averaged topic trajectories of participants' recalls (Fig. 7B). To assess the consistency  
292 of these recall trajectories across participants, we asked: given that a participant's recall trajectory  
293 had entered a particular location in topic space, could the position of their *next* recalled event  
294 be predicted reliably? For each location in topic space, we computed the set of line segments  
295 connecting successively recalled events (across all participants) that intersected that location (see  
296 *Methods* for additional details). We then computed (for each location) the distribution of angles  
297 formed by the lines defined by those line segments and a fixed reference line (the *x*-axis). Rayleigh  
298 tests revealed the set of locations in topic space at which these across-participant distributions  
299 exhibited reliable peaks (blue arrows in Fig. 7B reflect significant peaks at  $p < 0.05$ , corrected). We  
300 observed that the locations traversed by nearly the entire video trajectory exhibited such peaks.  
301 In other words, participants exhibited similar trajectories that also matched the trajectory of the  
302 original video (Fig. 7C). This is especially notable when considering the fact that the number of  
303 events participants recalled (dots in Fig. 7C) varied considerably across people, and that every  
304 participant used different words to describe what they had remembered happening in the video.  
305 Differences in the numbers of remembered events appear in participants' trajectories as differences  
306 in the sampling resolution along the trajectory. We note that this framework also provides a  
307 means of disentangling classic "proportion recalled" measures (i.e., the proportion of video events  
308 described in participants' recalls) from participants' abilities to recapitulate the overall unfolding  
309 of the original video's content (i.e., the similarity between the shapes of the original video trajectory  
310 and that defined by each participant's recounting of the video).

311 The results displayed in Figures 3C and 5A suggest that certain events were remembered better

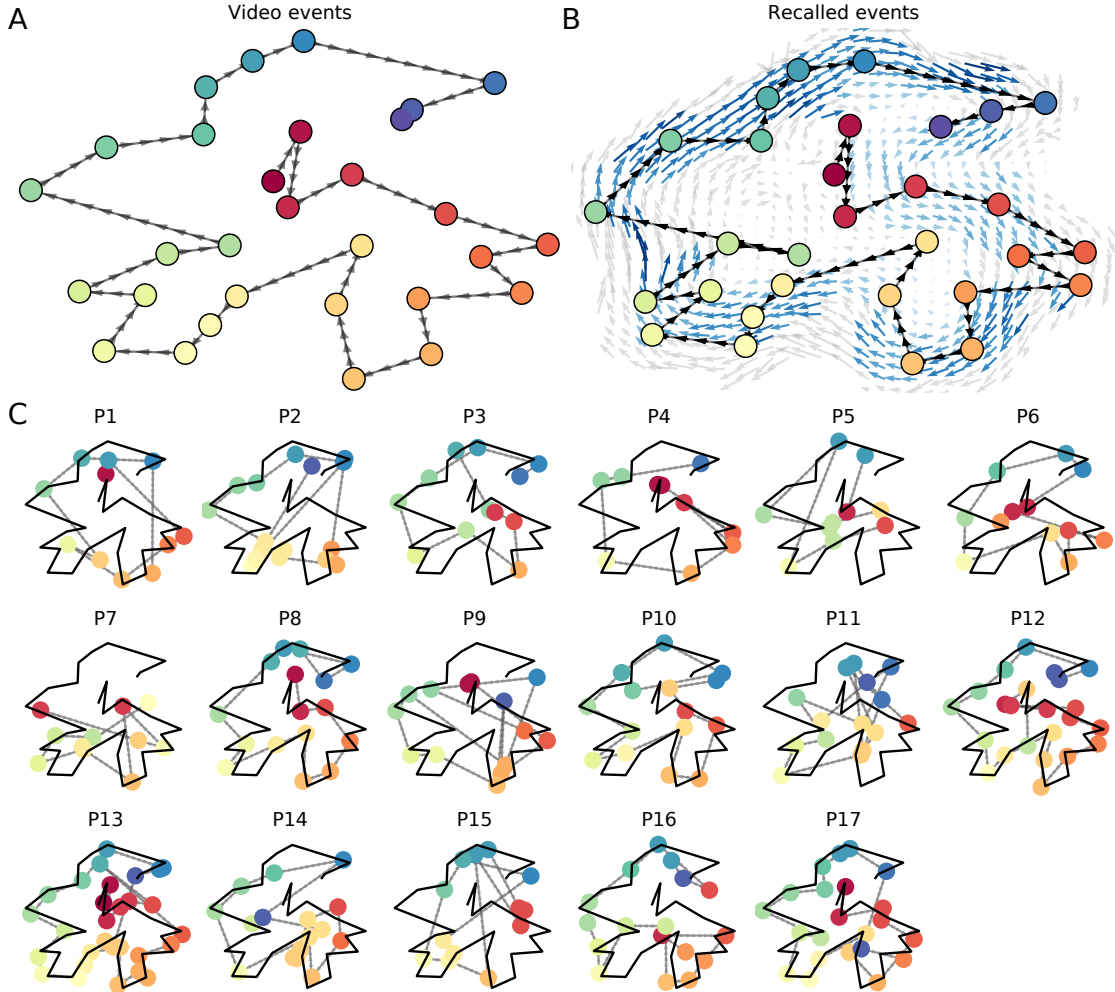


**Figure 7: Trajectories through topic space capture the dynamic content of the video and recalls.** All panels: the topic proportion matrices have been projected onto a shared two-dimensional space using UMAP. **A.** The two-dimensional topic trajectory taken by the episode of *Sherlock*. Each dot indicates an event identified using the HMM (see *Methods*); the dot colors denote the order of the events (early events are in red; later events are in blue), and the connecting lines indicate the transitions between successive events. **B.** The average two-dimensional trajectory captured by participants' recall sequences, with the same format and coloring as the trajectory in Panel A. To compute the event positions, we matched each recalled event with an event from the original video (see *Results*), and then we averaged the positions of all events with the same label. The arrows reflect the average transition direction through topic space taken by any participants whose trajectories crossed that part of topic space; blue denotes reliable agreement across participants via a Rayleigh test ( $p < 0.05$ , corrected). **C.** The recall topic trajectories (gray) taken by each individual participant (P1–P17). The video's trajectory is shown in black for reference. Here, events (dots) are colored by their matched video event (Panel A).

than others. Given this, we next asked whether the events were generally remembered well or poorly tended to reflect particular content. Because our analysis framework projects the dynamic video content and participants' recalls into a shared space, and because the dimensions of that space represent topics (which are, in turn, sets of weights over words in the vocabulary), we are able to recover the weighted combination of words that make up any point (i.e., topic vector) in this space. We first computed the average precision with which participants recalled each of the 30 video events (Fig. 8A; note that this result is analogous to a serial position curve created from our continuous recall quality metric). We then computed a weighted average of the topic vectors for each video event, where the weights reflected how reliably each event was recalled. To visualize the result, we created a "wordle" image (Mueller et al., 2018) where words weighted more heavily by better-remembered topics appear in a larger font (Fig. 8B, green box). Across the full video, content that reflected topics necessary to convey the central focus of the video (e.g., the names of the two main characters, "Sherlock" and "John", and the address of a major recurring location, "221B Baker Street") were best remembered. An analogous analysis revealed which themes were poorly remembered. Here in computing the weighted average over events' topic vectors, we weighted each event in *inverse* proportion to how well it was remembered (Fig. 8B, red box). The least well-remembered video content reflected information not necessary to later convey a general summary of the video, such as the proper names of relatively minor characters (e.g., "Mike," "Molly," and "Lestrade") and locations (e.g., "St. Bartholomew's Hospital").

A similar result emerged from assessing the topic vectors for individual video and recall events (Fig. 8C). Here, for each of the three best- and worst-remembered video events, we have constructed two wordles: one from the original video event's topic vector (left) and a second from the average recall topic vector for that event (right). The three best-remembered events (circled in green) correspond to scenes important to the central plot-line: a mysterious figure spying on John in a phone booth; John meeting Sherlock at Baker St. to discuss the murders; and Sherlock laying a trap to catch the killer. Meanwhile, the three worst-remembered events (circled in red) reflect scenes that are non-essential to summarizing the narrative's structure: the video of singing cartoon characters participants viewed prior to the main episode; John asking Molly about Sherlock's habit

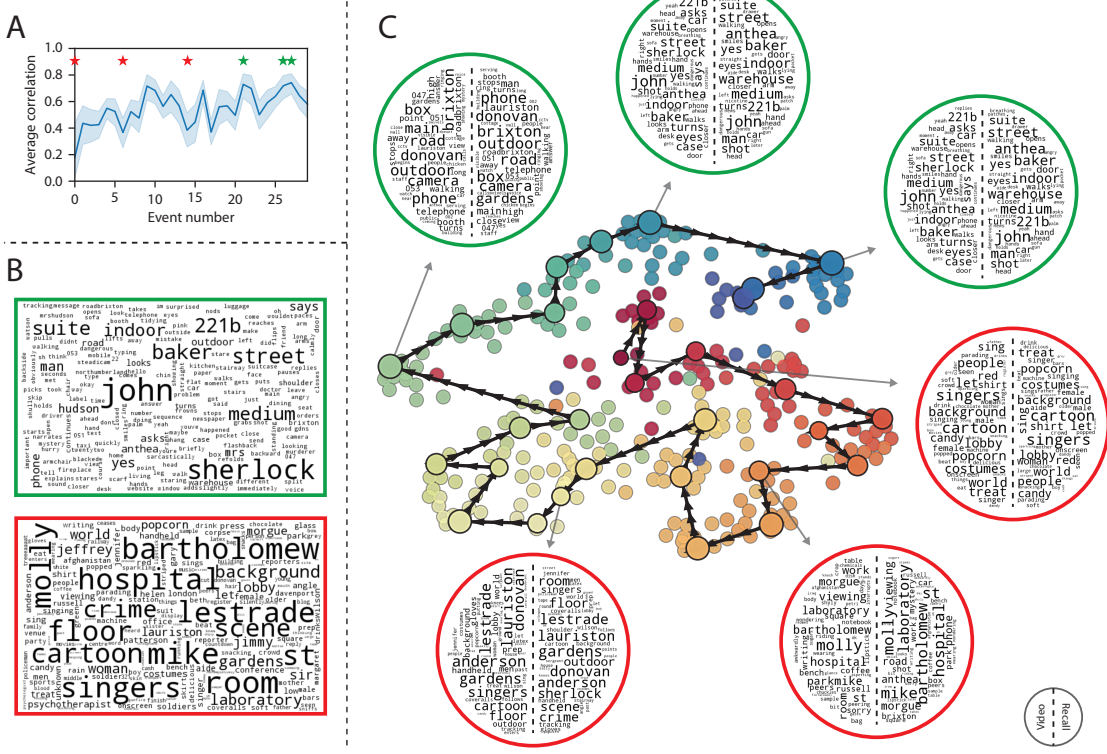


**Figure 8: Transforming experience into memory.** **A.** Average precision (video event-recall event topic vector correlation) across participants for each video event. Error bars denote bootstrap-derived across-participant 95% confidence intervals. The stars denote the three best-remembered events (green) and worst-remembered events (red). **B.** Wordles comprising the top 200 highest-weighted words reflected in the weighted-average topic vector across video events. Green: video events were weighted by how well the topic vectors derived from recalls of those events matched the video events' topic vectors (Panel A). Red: video events were weighted by the inverse of how well their topic vectors matched the recalled topic vectors. **C.** The set of all video and recall events is projected onto the two-dimensional space derived in Figure 7. The dots outlined in black denote video events (dot size reflects the average correlation between the video event's topic vector and the topic vectors from the closest matching recalled events from each participant; bigger dots denote stronger correlations). The dots without black outlines denote recalled events. All dots are colored using the same scheme as Figure 7A. Wordles for several example events are displayed (green: three best-remembered events; red: three worst-remembered events). Within each circular wordle, the left side displays words associated with the topic vector for the video event, and the right side displays words associated with the (average) recall event topic vector, across all recall events matched to the given video event.

340 of over-analyzing people; and Sherlock noticing evidence of Anderson's and Donovan's affair.

341 The results thus far inform us about which aspects of the dynamic content in the episode partic-  
342 ipants watched were preserved or altered in participants' memories. We next carried out a series  
343 of analyses aimed at understanding which brain structures might facilitate these preservations and  
344 transformations between the external world and memory. In one analysis, we sought to identify  
345 brain structures that were sensitive to the dynamic unfolding of the video's content, as character-  
346 ized by its topic trajectory. We used a searchlight procedure to identify clusters of voxels whose  
347 activity patterns displayed a proximal temporal correlation structure (as participants watched the  
348 video) matching that of the original video's topic proportions (Fig. 9A; see *Methods* for additional  
349 details). In a second analysis, we sought to identify brain structures whose responses (during video  
350 viewing) reflected how each participant would later structure their *recalls* of the video. We used an  
351 analogous searchlight procedure to identify clusters of voxels whose proximal temporal correlation  
352 matrices matched that of the topic proportions for each individual's recall (Figs. 9B; see *Methods* for  
353 additional details). To ensure our searchlight procedure identified regions *specifically* sensitive to  
354 the temporal structure of the video or recalls (i.e., rather than those with a temporal autocorrelation  
355 length similar to that of the video/recalls), we performed a phase shift-based permutation correc-  
356 tion (see *Methods* for additional details). Specifically, we circularly shifted the timeseries of the  
357 topic trajectory by a random number of timepoints, recomputed the shifted trajectory's correlation  
358 matrix, and again performed our searchlight analysis on this permuted data. We then z-scored  
359 the "real" searchlight results at each voxel against the null distribution of (100) permuted results.  
360 In Figure 9, only voxels whose activity pattern reflected the "real" video/recall timeseries more  
361 closely than 95% of the permuted results are shown. As shown in Figure 9C, the video-driven  
362 searchlight analysis revealed a distributed network of regions including ????, suggesting that these  
363 regions may play a role in processing information relevant to the narrative structure of the video.  
364 As shown in Figure 9D, the analysis revealed a network of regions including ????, suggesting  
365 that these regions facilitate a person-specific transformation of one's experience into memory. In  
366 identifying regions whose responses to ongoing experiences reflect how those experiences will be  
367 remembered later, this latter analysis extends classic *subsequent memory analyses* (e.g., Paller and

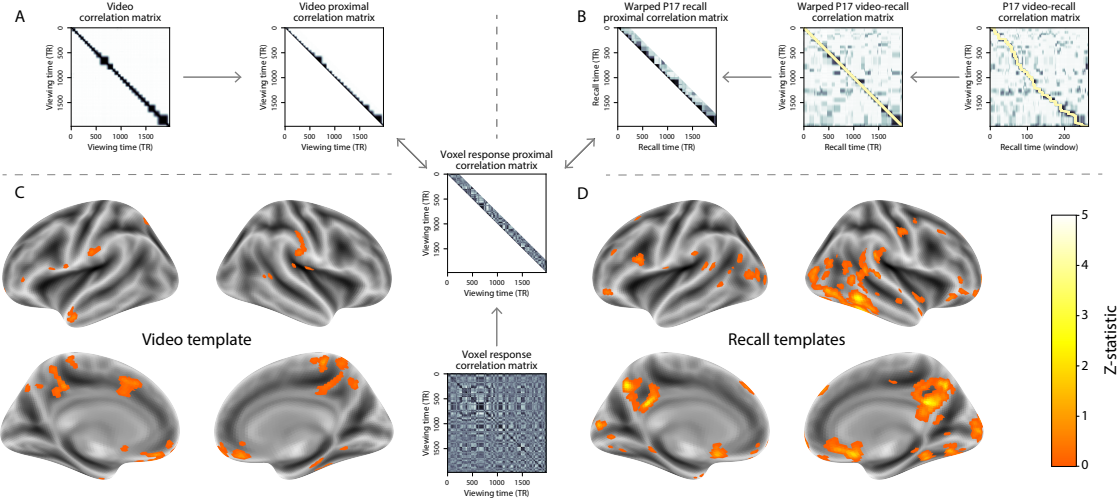


**Figure 9: Brain structures that underlie the transformation of experience into memory.** **A.** We isolated the proximal diagonals from the upper triangle of the video correlation matrix, and applied this same diagonal mask to the voxel response correlation matrix for each cube of voxels in the brain. We then searched for brain regions whose activation timeseries consistently exhibited a similar proximal correlational structure to the video model, across participants. **B.** We used dynamic time warping (Berndt and Clifford, 1994) to align each participant's recall timeseries to the TR timeseries of the video. We then applied the same diagonal mask used in Panel A to isolate the proximal temporal correlations and searched for brain regions whose activation timeseries for an individual consistently exhibited a similar proximal correlational structure to each individual's recall. **C.** We identified a network of regions sensitive to the narrative structure of participants' ongoing experience. The map shown is thresholded at  $p < 0.05$ , corrected. **D.** We also identified a network or regions sensitive to how individuals would later structure the video's content in their recalls. The map shown is thresholded at  $p < 0.05$ , corrected.

368 Wagner, 2002) to domain of naturalistic stimuli.

369 The searchlight analyses described above yielded two distributed networks of brain regions,  
 370 whose activity timecourses mirrored to the temporal structure of the video (Fig. 9C) or participants'  
 371 eventual recalls (Fig. 9D). We next sought to gain greater insight into the structures and  
 372 functional networks our results reflected. To accomplish this in a blind, unbiased manner (i.e.,  
 373 without reverse inference via visual observation) we performed an additional, exploratory analy-  
 374 sis using Neurosynth (Yarkoni et al., 2011). Neurosynth parses a massive online database of over  
 375 14,000 neuroimaging studies and constructs meta-analysis images for over 13,000 psychology-  
 376 and neuroscience-related terms, based on NIfTI images accompanying studies where those terms  
 377 appear at a high frequency. Then, given a novel image (tagged with its value type; e.g.,  $t$ -,  $F$ - or

378 *p*-statistics), Neurosynth returns a list of terms whose meta-analysis images are most similar to this  
379 new data. Our permutation procedure (described above) yielded, for each of the two searchlight  
380 analyses, a voxelwise map of significance (*p*-statistic) values. These maps describe the extent to  
381 which each voxel *specifically* reflected the temporal structure of the video or individuals' recalls (i.e.,  
382 for each voxel, the proportion of phase-shifted topic vector correlation matrices less similar to the  
383 voxel activity correlation matrix than the unshifted video's correlation matrix). These significance  
384 maps for the video- and recall-driven searchlight analyses, along with the 10 terms with maximally  
385 similar meta-analysis images identified by Neurosynth are shown in Figure 10.

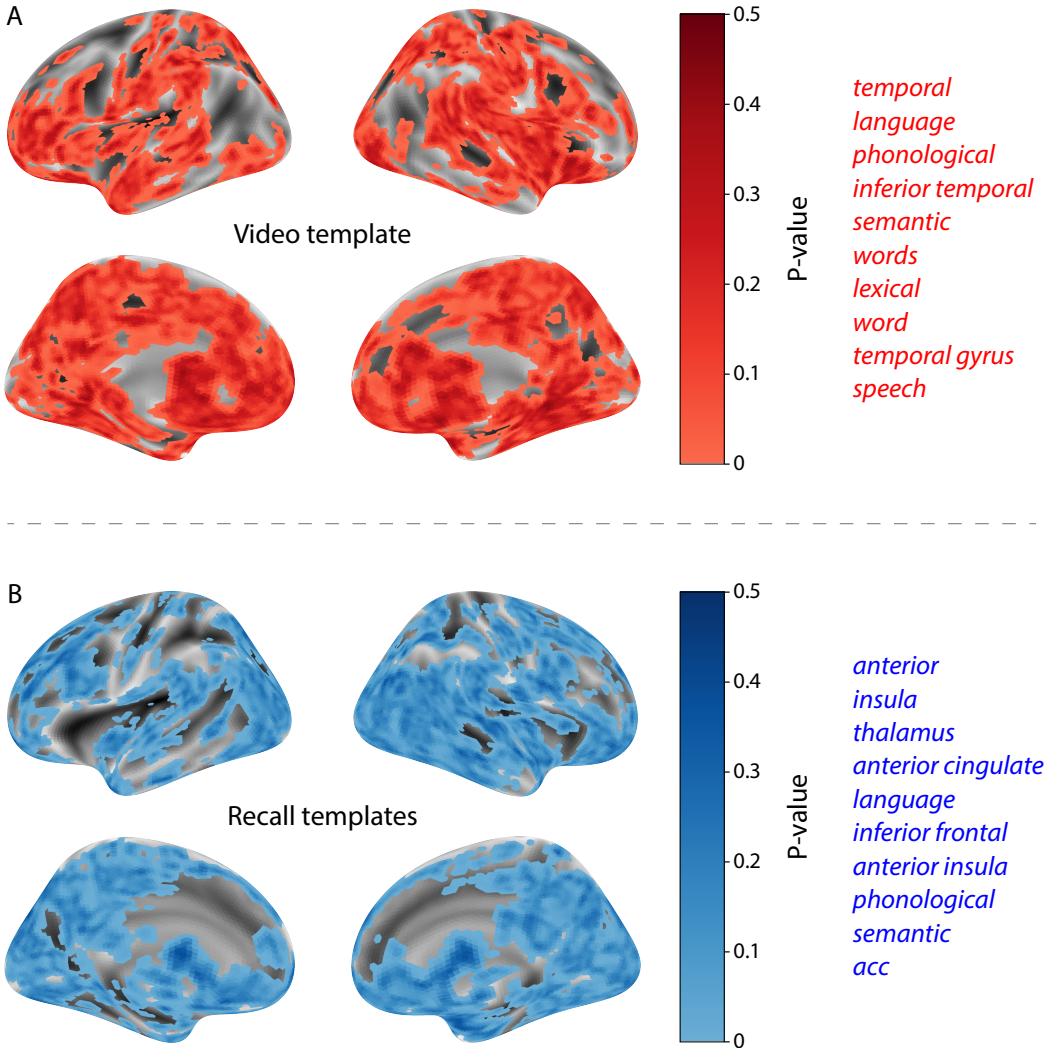


**Figure 10: Decoding distributed statistical maps via Neurosynth meta-analyses.** **A.** Video-searchlight significance and top 10 decoded terms. We constructed a map of the permutation-derived  $p$ -values for the video-driven searchlight analysis (Fig. 9A, C) at each voxel with a positive permutation-derived  $z$ -score. The top 10 terms decoded from this significance map are shown in red. **B.** Recall-searchlight significance and top 10 decoded terms. We constructed a map of the permutation-derived  $p$ -values for the recall-driven searchlight analysis (Fig. 9A, C) at each voxel with a positive permutation-derived  $z$ -score. The top 10 terms decoded from this significance map are shown in blue.

386 **Discussion**

387 Our work casts remembering as reproducing (behaviorally and neurally) the topic trajectory, or  
388 shape, of an experience. This view draws inspiration from prior work aimed at elucidating  
389 the neural and behavioral underpinnings of how we process dynamic naturalistic experiences  
390 and remember them later. One approach to identifying neural responses to naturalistic stimuli  
391 (including experiences) entails building a model of the stimulus and searching for brain regions  
392 whose responses are consistent with the model. In prior work, a series of studies from Uri  
393 Hasson’s group (Lerner et al., 2011; Simony et al., 2016; Chen et al., 2017; Baldassano et al., 2017;  
394 Zadbood et al., 2017) have extended this approach with a clever twist: rather than building an  
395 explicit stimulus model, these studies instead search for brain responses (while experiencing the  
396 stimulus) that are reliably similar across individuals. So called *inter-subject correlation* (ISC) and  
397 *inter-subject functional connectivity* (ISFC) analyses effectively treat other people’s brain responses  
398 to the stimulus as a “model” of how its features change over time. By contrast, in our present work  
399 we used topic models to construct an explicit content model directly from the stimulus (i.e., the  
400 topic trajectory of the video). Projecting each participant’s recall into a space shared by both the  
401 stimulus and other participants then allows us to compare recalls both directly to the stimulus and  
402 to each other. Similarly, prior work introducing the use of HMMs to discover latent event structure  
403 in naturalistic stimuli and recall (Baldassano et al., 2017) used a between-subjects cross-validation  
404 approach to identify event boundaries shared across participants, and between stimulus and recall.  
405 Our framework allows us to break from the restriction of a common, shared event-timeseries and  
406 identify the unique *resolution* of each participant’s recall event structure, and how that may differ  
407 from the video and each other.

408 In extending classical free recall analyses to our naturalistic memory framework, we recovered  
409 two patterns of recall dynamics central to list-learning studies: a heightened probability of initiating  
410 recall with the first presented “item” (in our case, video events; Fig. 3A) and a strong bias toward  
411 transitioning from recalling a given event to recalling the one immediately following it (Fig. 3B).  
412 However, equally noteworthy are the typical free recall results *not* recovered in these analyses,

as each highlights a fundamental difference between the list-learning paradigm and naturalistic memory paradigms like the one employed in the present study. The most noticeable departure from hallmark free recall dynamics in these findings is the apparent lack of a serial position effect in Figure 3C, which instead shows greater and lesser recall probabilities for events distributed across the video. Stimuli in free recall experiments most often comprise lists of simple, common words, presented to participants in a random order. (In fact, numerous word pools have been developed based on these criteria; e.g., Friendly et al., 1982). These stimulus qualities enable two assumptions that are central to word list analyses, but frequently do not hold for real-world experiences. First, researchers conducting free recall studies may assume that the content at each presentation index is essentially equal, and does not possess attributes that would render it, on average, more or less memorable than others. Such is rarely the case with real-world experiences or experiments meant to approximate them, and the effects of both intrinsic and observer-dependent factors on stimulus memorability are well established (for review see Chun and Turk-Browne, 2007; Bylinskii et al., 2015; Tyng et al., 2017). Second, the random ordering of list items ensures that (across participants, on average) there is no relationship between the thematic similarity of individual stimuli and their presentation positions—in other words, two successively presented items are no more likely to be highly semantically similar than they are to be high dissimilar. In most cases, the exact opposite is true of real-world episodes. Our internal thoughts, our actions, and the physical state of the world around us all tend to follow a direct, causal progression. As a result, each moment of our experience tends to be inherently more similar to surrounding moments than to those in the distant past or future. Memory literature has termed this strong temporal autocorrelation “context,” and in various media that depict real-world events (e.g., movies or written stories), we recognize it as a *narrative structure*. While a random word list (by definition) has no such structure, the logical progression between ideas and actions in a naturalistic stimulus prompts the rememberer to recount presented events in order, starting with the beginning. This tendency is reflected in our findings’ second departure from typical free recall dynamics: a lack of increased probability of first recall for end-of-sequence events (Fig. 3A).

Because they disregard presentation order-dependent variability in the stimulus content, anal-

yses such as those in Figure 3 enable a more sensitive analysis of presentation order-dependent temporal dynamics in free recall. Yet by the same token, they paint a wholly incomplete picture of memory for naturalistic episodes. In an attempt to address this shortcoming, we have developed a framework in the present study that characterizes the explicit semantic content of the stimulus and subsequent recalls. However, sensitivity to stimulus and recall content introduces a new challenge: distinguishing between levels of recall quality for a stimulus (e.g., an event) that is considered to have been “remembered.” When modeling memory in an experimental setting, recall quality for individual events is often cast as binary (e.g., a given list item was simply either remembered or not remembered). Various models of memory (e.g., Yonelinas, 2002) attempt to improve upon this by including confidence ratings, rendering this binary judgement instead categorical. To better evaluate naturalistic memory quality, we introduce a continuous metric (*precision*), which reflects the level of completeness of a participant’s recall for a feature-rich experience. Additionally, recall quality for a single event is typically assessed independently from that for all other events (e.g., it is difficult to “compare” a participant’s binary recall success for list item 1 to that of list item 10). The second novel metric we introduce (*distinctiveness*) is based on analyzing of the correlational structure of an individual’s full set of recall events, and reflects the specificity of their memory for a single experienced event. We find that both of these metrics relate to the overall number of video events participants successfully recalled, and that our precision metric additionally relates to Chen et al. (2017)’s hand-annotated memory scores. Though we do not find participants’ average recall distinctiveness related to the hand-annotated memory scores, this is not entirely surprising given the divergence of behavior they capture. In hand-scoring each participant’s verbal recall for each of 50 (manually-delimited) scenes, “[a] scene was counted as recalled if the participant described any part of the scene” (Chen et al., 2017). In other words, both an extensive description of a scene’s content and a brief mention of some subset of its content were (binarily) considered equally successful recalls. By contrast, we identify the event structure in participants’ recalls in an unsupervised manner, independent of the video event-timeseries, prior to mapping between video and recall content. Our HMM-based event-segmentation produces boundaries between timepoints where the topic proportions shift in a substantial way, and because a small

469 handful of words is unlikely to contribute significantly to the topic proportions for any sliding win-  
470 dow, such brief scene descriptions will most often not begat a sufficiently large shift in the resulting  
471 topic proportions for the HMM to identify an event boundary. Instead, they will be grouped with  
472 a neighboring event, consequently lowering that event’s distinctiveness score and by extension,  
473 the participant’s overall distinctiveness score. This is in essence the qualitative difference between  
474 distinctive and indistinctive recall, and reflects the comparison shown in Figure 6C. Intriguingly,  
475 prior studies show that pattern separation, or the ability to cleanly discriminate between similar  
476 experiences, is impaired in many cognitive disorders as well as natural aging (Stark et al., 2010;  
477 Yassa et al., 2011; Yassa and Stark, 2011). Future work might explore whether and how these  
478 metrics compare between cognitively impoverished groups and healthy controls.

479 While a large number of language models exist (e.g., WAS, LSA, word2vec, universal sentence  
480 encoder; Steyvers et al., 2004; Landauer et al., 1998; Mikolov et al., 2013; Cer et al., 2018), here  
481 we use latent dirichlet allocation (LDA)-based topic models for a few reasons. First, topic models  
482 capture the *essence* of a text passage devoid of the specific set and order of words used. This was  
483 an important feature of our model since different people may accurately recall a scene using very  
484 different language. Second, words can mean different things in different contexts (e.g. “bat” may  
485 be the act of hitting a baseball, the object used for that action, or as a flying mammal). Topic  
486 models are robust to this, allowing words to exist as part of multiple topics. Last, topic models  
487 provide a straightforward means to recover the weights for the particular words comprising a topic,  
488 enabling easy interpretation of an event’s contents (e.g. Fig. 8). Other models such as Google’s  
489 Universal Sentence Encoder offer a context-sensitive encoding of text passages, but the encoding  
490 space is complex and non-linear, and thus recovering the original words used to fit the model is  
491 not straightforward. However, it’s worth pointing out that our framework is divorced from the  
492 particular choice of language model. Moreover, many of the aspects of our framework could be  
493 swapped out for other choices. For example, the language model, the timeseries segmentation  
494 model and the video-recall matching function could all be customized for the particular problem.  
495 Indeed for some problems, recovery of the particular recall words may not be necessary, and thus  
496 other text-modeling approaches (such as universal sentence encoder) may be preferable. Future

497 work will explore the influence of particular model choices on the framework's efficacy.

498 In the analyses outlined in Figure 9, we identified two diffuse networks of brain structures whose  
499 responses were consistent with the video and recall topic trajectories, respectively. Decoding the  
500 associated significance maps with Neurosynth revealed two intriguing results. First, the top 10  
501 terms returned for the video-driven searchlight significance map were centered around themes of  
502 language and semantic meaning (Fig. 10A). In other words, the voxels identified as more reflective  
503 of the video's temporal structure (i.e., voxels with lower permutation correction-derived  $p$ -values),  
504 as defined by our model, were most likely to be reported as active in studies focused on the the  
505 neural underpinnings of semantic processing. This finding is interesting, as our model specifically  
506 captures the temporal structure of the video's *semantic* content (e.g., as opposed to that of the  
507 visual, auditory, or affective content). This suggests that the network of structures displayed in  
508 Figure 9C may play a role in processing the evolving semantic structure of ongoing experiences.

509 Our second searchlight analysis identified a largely separate network of regions (Fig. 9D)  
510 whose patterns of activity as participants viewed the video reflected the idiosyncratic structure  
511 of each individual's later recall. Decoding the associated significance map yielded a set of terms  
512 that primarily reflected names of specific structural regions (such as "thalamus," "anterior insula,"  
513 "anterior cingulate" and "inferior frontal"; Fig. 10B). Interestingly, these regions share membership  
514 in a common, large-scale functional network (termed the "salience network") involved in detect-  
515 ing and processing affective cues. In particular, the latter three regions have been implicated in  
516 functions relevant to assigning personal meaning to an experience, including: ascribing subjective  
517 value to raw, sensory input (Medford and Critchley, 2010); modulating semantic and phonological  
518 processing in response to personally salient stimuli (Kelly et al., 2007); and directing and reallo-  
519 cating attention and working memory resources towards the most relevant stimuli (Menon and  
520 Uddin, 2010). This suggests that the network of structures displayed in Figure 9D may be play a  
521 roll in transforming and restructuring ongoing experiences through the lens of one's own personal  
522 values as they are encoded in memory.

523 Our work has broad implications for how we characterize and assess memory in real-world  
524 settings, such as the classroom or physician's office. For example, the most commonly used

525 classroom evaluation tools involve simply computing the proportion of correctly answered exam  
526 questions. Our work indicates that this approach is only loosely related to what educators might  
527 really want to measure: how well did the students understand the key ideas presented in the  
528 course? Under this typical framework of assessment, the same exam score of 50% could be  
529 ascribed to two very different students: one who attended the full course but struggled to learn  
530 more than a broad overview of the material, and one who attended only half of the course but  
531 understood the material perfectly. Instead, one could apply our computational framework to build  
532 explicit content models of the course material and exam questions. This approach would provide  
533 a more nuanced and specific view into which aspects of the material students had learned well  
534 (or poorly). In clinical settings, memory measures that incorporate such explicit content models  
535 might also provide more direct evaluations of patients' memories.

## 536 Methods

### 537 Experimental design and data collection

538 Data were collected by Chen et al. (2017). In brief, participants ( $n = 22$ ) viewed the first 48 minutes  
539 of "A Study in Pink", the first episode of the BBC television series *Sherlock*, while fMRI volumes  
540 were collected (TR = 1500 ms). Participants were pre-screened to ensure they had never seen any  
541 episode of the show before. The stimulus was divided into a 23 min (946 TR) and a 25 min (1030 TR)  
542 segment to mitigate technical issues related to the scanner. After finishing the clip, participants  
543 were instructed to (quoting from Chen et al., 2017) "describe what they recalled of the [episode]  
544 in as much detail as they could, to try to recount events in the original order they were viewed  
545 in, and to speak for at least 10 minutes if possible but that longer was better. They were told that  
546 completeness and detail were more important than temporal order, and that if at any point they  
547 realized they had missed something, to return to it. Participants were then allowed to speak for  
548 as long as they wished, and verbally indicated when they were finished (e.g., 'I'm done')." Five  
549 participants were dropped from the original dataset due to excessive head motion (2 participants),

550 insufficient recall length (2 participants), or falling asleep during stimulus viewing (1 participant),  
551 resulting in a final sample size of  $n = 17$ . For additional details about the experimental procedure  
552 and scanning parameters, see Chen et al. (2017). The experimental protocol was approved by  
553 Princeton University's Institutional Review Board.

554 After preprocessing the fMRI data and warping the images into a standard ( $3 \text{ mm}^3$  MNI) space,  
555 the voxel activations were z-scored (within voxel) and spatially smoothed using a 6 mm (full width  
556 at half maximum) Gaussian kernel. The fMRI data were also cropped so that all video-viewing  
557 data were aligned across participants. This included a constant 3 TR (4.5 s) shift to account for the  
558 lag in the hemodynamic response. (All of these preprocessing steps followed Chen et al., 2017,  
559 where additional details may be found.)

560 The video stimulus was divided into 1,000 fine-grained “scenes” and annotated by an inde-  
561 pendent coder. For each of these 1,000 scenes, the following information was recorded: a brief  
562 narrative description of what was happening, the location where the scene took place, whether  
563 that location was indoors or outdoors, the names of all characters on-screen, the name(s) of the  
564 character(s) in focus in the shot, the name(s) of the character(s) currently speaking, the camera  
565 angle of the shot, a transcription of any text appearing on-screen, and whether or not there was  
566 music present in the background. Each scene was also tagged with its onset and offset time, in  
567 both seconds and TRs.

## 568 **Data and code availability**

569 The fMRI data we analyzed are available online [here](#). The behavioral data and all of our analysis  
570 code may be downloaded [here](#).

## 571 **Statistics**

572 All statistical tests performed in the behavioral analyses were two-sided. All statistical tests per-  
573 formed in the neural data analyses were two-sided, except for the permutation-based thresholding,  
574 which was one-sided. In this case, we were specifically interested in identifying voxels whose ac-

575 tivation time series reflected the temporal structure of the video and recall trajectories to a *greater*  
576 extent than that of the phase-shifted trajectories.

## 577 **Modeling the dynamic content of the video and recall transcripts**

### 578 **Topic modeling**

579 The input to the topic model we trained to characterize the dynamic content of the video comprised  
580 998 hand-generated annotations of short (mean: 2.96s) scenes spanning the video clip (Chen et al.,  
581 2017 generated 1000 annotations total; we removed two referring to the break between the first and  
582 second scan sessions, during which no fMRI data was collected). The features annotated included:  
583 narrative details (a sentence or two describing what happened in that scene); whether the scene  
584 took place indoors or outdoors; names of any characters that appeared in the scene; name(s) of  
585 characters in camera focus; name(s) of characters who were speaking in the scene; the location (in  
586 the story) that the scene took place; camera angle (close up, medium, long, top, tracking, over the  
587 shoulder, etc.); whether music was playing in the scene or not; and a transcription of any on-screen  
588 text. We concatenated the text for all of these features within each segment, creating a “bag of  
589 words” describing each scene. We then re-organized the text descriptions into overlapping sliding  
590 windows of 50 scenes each. In other words, we created a “context” for each scene comprising the  
591 text descriptions of the preceding 25 scenes, the present scene, and the following 24 scenes. To  
592 model the “context” at the beginning and end of the video (i.e., within 25 scenes of the beginning or  
593 end), we created overlapping sliding windows that grew in size from one scene to the full length,  
594 then similarly tapered their length at the end. This bore the additional benefit of representing each  
595 scene’s description in the text corpus an equal number of times.

596 We trained our model using these overlapping text samples with `scikit-learn` (version 0.19.1;  
597 Pedregosa et al., 2011), called from our high-dimensional visualization and text analysis software,  
598 `HyperTools` (Heusser et al., 2018b). Specifically, we used the `CountVectorizer` class to transform  
599 the text from each window into a vector of word counts (using the union of all words across all  
600 scenes as the “vocabulary,” excluding English stop words); this yielded a number-of-windows

601 by number-of-words *word count* matrix. We then used the `LatentDirichletAllocation` class  
602 (`topics=100, method='batch'`) to fit a topic model (Blei et al., 2003) to the word count matrix,  
603 yielding a number-of-windows (1047) by number-of-topics (100) *topic proportions* matrix. The  
604 topic proportions matrix describes which mix of topics (latent themes) is present in and around  
605 each scene. Next, we transformed the topic proportions matrix to match the 1976 fMRI volume  
606 acquisition times. We assigned each topic vector to the timepoint midway between the beginning  
607 of the first scene and the end of the last scene in its corresponding sliding text window. We  
608 then transformed these timepoints to units of TRs and interpolated the dynamic topic proportions  
609 matrix to obtain number-of-TRs (1976) by number-of-topics (100) matrix.

610 We created similar topic proportions matrices using hand-annotated transcripts of each partici-  
611 pant's recall of the video (annotated by Chen et al., 2017). We tokenized the transcript into a list of  
612 sentences, and then re-organized the list into overlapping sliding windows spanning 10 sentences  
613 each (and analogously tapered the lengths of the first and last 10 sliding windows). In turn, we  
614 transformed each window's sentences into a word count vector (using the same vocabulary as for  
615 the video model). We then used the topic model already trained on the video scenes to compute  
616 the most probable topic proportions for each sliding window. This yielded a number-of-windows  
617 (range: 83–312) by number-of-topics (100) topic proportions matrix for each participant. These  
618 reflected the dynamic content of each participant's recalls. Note: for details on how we selected the  
619 video and recall window lengths and number of topics, see *Supporting Information* and Figure S1.

## 620 **Parsing topic trajectories into events using Hidden Markov Models**

621 We parsed the topic trajectories of the video and participants' recalls into events using Hidden  
622 Markov Models (Rabiner, 1989). Given the topic proportions matrix (describing the mix of topics  
623 at each timepoint) and a number of states,  $K$ , an HMM recovers the set of state transitions that  
624 segments the timeseries into  $K$  discrete states. Following Baldassano et al. (2017), we imposed an  
625 additional set of constraints on the discovered state transitions that ensured that each state was  
626 encountered exactly once (i.e., never repeated). We used the BrainIAK toolbox (Capota et al., 2017)  
627 to implement this segmentation.

628 We used an optimization procedure to select the appropriate  $K$  for each topic proportions  
629 matrix. Prior studies on narrative structure and processing have shown that we both perceive  
630 and internally represent the world around us at multiple, hierarchical timescales (e.g., Hasson  
631 et al., 2008; Lerner et al., 2011; Hasson et al., 2015; Chen et al., 2017; Baldassano et al., 2017, 2018).  
632 However, for the purposes of our framework, we sought to identify the single timescale of event-  
633 representations that is emphasized *most heavily* in the temporal structure of the video and each  
634 participant's recalls. We quantified this as the set of  $K$  event boundaries that yielded the maximal  
635 distinctiveness between the content (i.e., topics) within each event and that in all other events.  
636 Specifically, we computed (for each matrix)

$$\operatorname{argmax}_K [W_1(a, b)],$$

637 where  $a$  was the distribution of correlations between the topic vectors of timepoints within the  
638 same state and  $b$  was the average correlation between the topic vectors of timepoints within  
639 *different* states. For each possible  $K$ , we computed the first Wasserstein distance ( $W_1$ ; also known as  
640 "earth mover's distance"; Dobrushin, 1970; Ramdas et al., 2017) between these distributions, and  
641 chose the  $K$ -value that yielded the greatest difference. Figure 2B displays the event boundaries  
642 returned for the video, and Figure S4 displays the event boundaries returned for each participant's  
643 recalls (See Fig. S6 for the optimization functions for the video and recalls). After obtaining these  
644 event boundaries, we created stable estimates of each topic proportions matrix by averaging the  
645 topic vectors within each event. This yielded a number-of-events by number-of-topics matrix for  
646 the video and recalls from each participant.

#### 647 **Naturalistic extensions of classic list-learning analyses**

648 In traditional list-learning experiments, participants view a list of items (e.g., words) and then recall  
649 the items later. Our video-recall event matching approach affords us the ability to analyze memory  
650 in a similar way. The video and recall events can be treated analogously to studied and recalled  
651 "items" in a list-learning study. We can then extend classic analyses of memory performance and

652 dynamics (originally designed for list-learning experiments) to the more naturalistic video recall  
653 task used in this study.

654 Perhaps the simplest and most widely used measure of memory performance is *accuracy*—i.e.,  
655 the proportion of studied (experienced) items (in this case, the 30 video events) that the participant  
656 later remembered. Chen et al. (2017) developed a human rating system whereby the quality of  
657 each participant’s memory was evaluated by an independent rater. We found a strong across-  
658 participants correlation between these independant ratings and the overall number of events that  
659 our HMM approach identified in participants’ recalls (Pearson’s  $r(15) = 0.65, p = 0.004$ ).

660 As described below, we next considered a number of memory performance measures that are  
661 typically associated with list-learning studies. We also provide a software package, Quail, for  
662 carrying out these analyses (Heusser et al., 2017).

663 **Probability of first recall (PFR).** PFR curves (Welch and Burnett, 1924; Postman and Phillips,  
664 1965; Atkinson and Shiffrin, 1968) reflect the probability that an item will be recalled first as a  
665 function of its serial position during encoding. To carry out this analysis, we initialized a number-  
666 of-participants (17) by number-of-video-events (30) matrix of zeros. Then for each participant, we  
667 found the index of the video event that was recalled first (i.e., the video event whose topic vector  
668 was most strongly correlated with that of the first recall event) and filled in that index in the matrix  
669 with a 1. Finally, we averaged over the rows of the matrix, resulting in a 1 by 30 array representing  
670 the proportion of participants that recalled an event first, as a function of the order of the event’s  
671 appearance in the video (Fig. 3A).

672 **Lag conditional probability curve (lag-CRP).** The lag-CRP curve (Kahana, 1996) reflects the  
673 probability of recalling a given event after the just-recalled event, as a function of their relative  
674 positions (or *lag*). In other words, a lag of 1 indicates that a recalled event came immediately after  
675 the previously recalled event in the video, and a lag of -3 indicates that a recalled event came 3  
676 events before the previously recalled event. For each recall transition (following the first recall),  
677 we computed the lag between the current recall event and the next recall event, normalizing by

678 the total number of possible transitions. This yielded a number-of-participants (17) by number-  
679 of-lags (-29 to +29; 61 lags total) matrix. We averaged over the rows of this matrix to obtain a  
680 group-averaged lag-CRP curve (Fig. 3B).

681 **Serial position curve (SPC).** SPCs (Murdock, 1962) reflect the proportion of participants that  
682 remember each item as a function of the items' serial position during encoding. We initialized  
683 a number-of-participants (17) by number-of-video-events (30) matrix of zeros. Then, for each  
684 recalled event, for each participant, we found the index of the video event that the recalled event  
685 most closely matched (via the correlation between the events' topic vectors) and entered a 1 into  
686 that position in the matrix (i.e., for the given participant and event). This resulted in a matrix  
687 whose entries indicated whether or not each event was recalled by each participant (depending  
688 on whether the corresponding entires were set to one or zero). Finally, we averaged over the rows  
689 of the matrix to yield a 1 by 30 array representing the proportion of participants that recalled each  
690 event as a function of the order of the event's appearance in the video (Fig. 3C).

691 **Temporal clustering scores.** Temporal clustering describes participants' tendency to organize  
692 their recall sequences by the learned items' encoding positions. For instance, if a participant  
693 recalled the video events in the exact order they occurred (or in exact reverse order), this would  
694 yield a score of 1. If a participant recalled the events in random order, this would yield an expected  
695 score of 0.5. For each recall event transition (and separately for each participant), we sorted  
696 all not-yet-recalled events according to their absolute lag (i.e., distance away in the video). We  
697 then computed the percentile rank of the next event the participant recalled. We averaged these  
698 percentile ranks across all of the participant's recalls to obtain a single temporal clustering score  
699 for the participant.

700 **Semantic clustering scores.** Semantic clustering describes participants' tendency to recall seman-  
701 tically similar presented items together in their recall sequences. Here, we used the topic vectors  
702 for each event as a proxy for its semantic content. Thus, the similarity between the semantic  
703 content for two events can be computed by correlating their respective topic vectors. For each

recall event transition, we sorted all not-yet-recalled events according to how correlated the topic vector of the closest-matching video event was to the topic vector of the closest-matching video event to the just-recalled event. We then computed the percentile rank of the observed next recall. We averaged these percentile ranks across all of the participant's recalls to obtain a single semantic clustering score for the participant.

### 709 Novel naturalistic memory metrics

710 **Precision.** We tested whether participants who recalled more events were also more *precise* in  
711 their recollections. For each participant, we computed the average correlation between the topic  
712 vectors for each recall event and those of its closest-matching video event. This gave a single value  
713 per participant representing the average precision across all recalled events. We then Fisher's *z*-  
714 transformed these values and correlated them with both hand-annotated and model-derived (i.e.,  
715  $k$  or the number of events recovered by the HMM) memory performance.

716 **Distinctiveness.** We also considered the *distinctiveness* of each recalled event. That is, how  
717 uniquely a recalled event's topic vector matched a given video event topic vector, versus the  
718 topic vectors for the other video events. We hypothesized that participants with high memory  
719 performance might describe each event in a more distinctive way (relative to those with lower  
720 memory performance who might describe events in a more general way). To test this hypothesis  
721 we define a distinctiveness score for each recall event as

$$d(\text{event}) = 1 - \bar{c}(\text{event}),$$

722 where  $\bar{c}(\text{event})$  is the average correlation between the given recalled event's topic vector and the  
723 topic vectors from all video events *except* the best-matching video event. We then averaged these  
724 distinctiveness scores across all of the events recalled by the given participant. As above, we used  
725 Fisher's *z*-transformation before correlating these values with hand-annotated and model derived  
726 memory performance scores across-subjects.

727 **Visualizing the video and recall topic trajectories**

728 We used the UMAP algorithm (McInnes et al., 2018) to project the 100-dimensional topic space  
729 onto a two-dimensional space for visualization (Figs. 7, 8). Importantly, to ensure that all of  
730 the trajectories were projected onto the *same* lower dimensional space, we computed the low-  
731 dimensional embedding on a “stacked” matrix created by vertically concatenating the events-  
732 by-topics topic proportions matrices for the video, across-participants average recalls and all 17  
733 individual participants’ recalls. We then divided the rows of the result (a total-number-of-events  
734 by two matrix) back into separate matrices for the video topic trajectory and the trajectories for  
735 each participant’s recalls (Fig. 7). This general approach for discovering a shared low-dimensional  
736 embedding for a collections of high-dimensional observations follows Heusser et al. (2018b). Note:  
737 for further details on how we created this low-dimensional embedding space, see *Supporting*  
738 *Information*.

739 **Estimating the consistency of flow through topic space across participants**

740 In Figure 7B, we present an analysis aimed at characterizing locations in topic space that dif-  
741 ferent participants move through in a consistent way (via their recall topic trajectories). The  
742 two-dimensional topic space used in our visualizations (Fig. 7) comprised a  $60 \times 60$  (arbitrary  
743 units) square. We tiled this space with a  $50 \times 50$  grid of evenly spaced vertices, and defined a  
744 circular area centered on each vertex whose radius was two times the distance between adjacent  
745 vertices (i.e., 2.4 units). For each vertex, we examined the set of line segments formed by connecting  
746 each pair successively recalled events, across all participants, that passed through this circle. We  
747 computed the distribution of angles formed by those segments and the  $x$ -axis, and used a Rayleigh  
748 test to determine whether the distribution of angles was reliably “peaked” (i.e., consistent across  
749 all transitions that passed through that local portion of topic space). To create Figure 7B we drew  
750 an arrow originating from each grid vertex, pointing in the direction of the average angle formed  
751 by line segments that passed within its circular radius. We set the arrow lengths to be inversely  
752 proportional to the  $p$ -values of the Rayleigh tests at each vertex. Specifically, for each vertex we

753 converted all of the angles of segments that passed within 2.4 units to unit vectors, and we set  
754 the arrow lengths at each vertex proportional to the length of the (circular) mean vector. We also  
755 indicated any significant results ( $p < 0.05$ , corrected using the Benjamani-Hochberg procedure) by  
756 coloring the arrows in blue (darker blue denotes a lower  $p$ -value, i.e., a longer mean vector); all  
757 tests with  $p \geq 0.05$  are displayed in gray and given a lower opacity value.

## 758 **Searchlight fMRI analyses**

759 In Figure 9, we present two analyses aimed at identifying brain regions whose responses (as par-  
760 ticipants viewed the video) exhibited a particular temporal structure. We developed a searchlight  
761 analysis wherein we constructed a cube centered on each voxel (radius: 5 voxels) and for each  
762 of these cubes, computed the temporal correlation matrix of the voxel responses during video  
763 viewing. Specifically, for each of the 1976 volumes collected during video viewing, we correlated  
764 the activity patterns in the given cube with the activity patterns (in the same cube) collected during  
765 every other timepoint. This yielded a 1976 by 1976 correlation matrix for each cube.

766 Next, we constructed a series of “template” matrices: the first reflecting the timecourse of  
767 video’s topic trajectory, and the others reflecting that of each participant’s recall topic trajectory.  
768 To construct the video template, we computed the correlations between the topic proportions  
769 estimated for every pair of TRs (prior to segmenting the trajectory into discrete events; i.e., the  
770 correlation matrix shown in Figs. 2B and 9A). We constructed similar temporal correlation matrices  
771 for each participant’s recall topic trajectory (Figs. 2D, S4). However, to correct for length differences  
772 and potential non-linear transformations between viewing time and recall time, we first used  
773 dynamic time warping (Berndt and Clifford, 1994) to temporally align participants’ recall topic  
774 trajectories with the video topic trajectory. An example correlation matrix before and after warping  
775 is shown in Fig. 9B. This yielded a 1976 by 1976 correlation matrix for the video template and for  
776 each participant’s recall template.

777 To determine which (cubes of) voxel responses matched the video template, we correlated  
778 the upper triangle of the voxel correlation matrix for each cube with the upper triangle of the  
779 video template matrix (Kriegeskorte et al., 2008). This yielded, for each participant, a voxelwise

780 map of correlation values. We then performed a one-sample  $t$ -test on the distribution of (Fisher  
781  $z$ -transformed) correlations at each voxel, across participants. This resulted in a value for each  
782 voxel (cube), describing how reliably its timecourse mirrored that of the video.

783 We further sought to ensure that our analysis identified regions where the activations' temporal  
784 structure specifically reflected that of the video, rather than regions whose activity was simply  
785 autocorrelated at a width similar to the video template's diagonal. To achieve this, we used a phase  
786 shift-based permutation procedure, wherein we circularly shifted the video's topic trajectory by  
787 a random number of timepoints, computed the resulting "null" video template, and re-ran the  
788 searchlight analysis, in full. (For each of the 100 permutations, the same random shift was used for  
789 all participants). We  $z$ -scored the observed (unshifted) result at each voxel against the distribution  
790 of permutation-derived "null" results, and estimated a  $p$ -value by computing the proportion of  
791 shifted results that yielded larger values. To create the map in Figure 9A, we thresholded out  
792 any voxels whose similarity to the unshifted video's structure fell below the 95<sup>th</sup> percentile of the  
793 permutation-derived similarity results.

794 We used an analogous procedure to identify which voxels' responses reflected the recall tem-  
795 plates. For each participant, we correlated the upper triangle of the correlation matrix for each cube  
796 of voxels with their (time warped) recall correlation matrix. As in the video template analysis this  
797 yielded a voxelwise map of correlation coefficients per participant. However, whereas the video  
798 analysis compared every participant's responses to the same template, here the recall templates  
799 were unique for each participant. As in the analysis described above, we  $t$ -scored the (Fisher  
800  $z$ -transformed) voxelwise correlations, and used the same permutation procedure we developed  
801 for the video responses to ensure specificity to the recall timeseries and assign significance values.  
802 To create the map in Figure 9B we again thresholded out any voxels whose correspondence values  
803 fell below the 95<sup>th</sup> percentile of the permutation-derived null distribution.

804 **References**

- 805 Atkinson, R. C. and Shiffrin, R. M. (1968). Human memory: A proposed system and its control  
806 processes. In Spence, K. W. and Spence, J. T., editors, *The psychology of learning and motivation*,  
807 volume 2, pages 89–105. Academic Press, New York.
- 808 Baldassano, C., Chen, J., Zadbood, A., Pillow, J. W., Hasson, U., and Norman, K. A. (2017).  
809 Discovering event structure in continuous narrative perception and memory. *Neuron*, 95(3):709–  
810 721.
- 811 Baldassano, C., Hasson, U., and Norman, K. A. (2018). Representation of real-world event schemas  
812 during narrative perception. *Journal of Neuroscience*, 38(45):9689–9699.
- 813 Berndt, D. J. and Clifford, J. (1994). Using dynamic time warping to find patterns in time series. In  
814 *KDD workshop*, volume 10, pages 359–370.
- 815 Blei, D. M. and Lafferty, J. D. (2006). Dynamic topic models. In *Proceedings of the 23rd International  
816 Conference on Machine Learning*, ICML '06, pages 113–120, New York, NY, US. ACM.
- 817 Blei, D. M., Ng, A. Y., and Jordan, M. I. (2003). Latent dirichlet allocation. *Journal of Machine  
818 Learning Research*, 3:993 – 1022.
- 819 Brunec, I. K., Moscovitch, M. M., and Barense, M. D. (2018). Boundaries shape cognitive represen-  
820 tations of spaces and events. *Trends in Cognitive Sciences*, 22(7):637–650.
- 821 Bylinskii, Z., Isola, P., Bainbridge, C., Torralba, A., and Oliva, A. (2015). Intrinsic and extrinsic  
822 effects on image memorability. *Vision Research*, 116:165–178.
- 823 Capota, M., Turek, J., Chen, P.-H., Zhu, X., Manning, J. R., Sundaram, N., Keller, B., Wang, Y., and  
824 Shin, Y. S. (2017). Brain imaging analysis kit.
- 825 Cer, D., Yang, Y., Kong, S. Y., Hua, N., Limtiaco, N., John, R. S., Constant, N., Guajardo-Cespedes,  
826 M., Yuan, S., Tar, C., Sung, Y.-H., Strope, B., and Kurzweil, R. (2018). Universal sentence encoder.  
827 *arXiv*, 1803.11175.

- 828 Chen, J., Leong, Y. C., Honey, C. J., Yong, C. H., Norman, K. A., and Hasson, U. (2017). Shared  
829 memories reveal shared structure in neural activity across individuals. *Nature Neuroscience*,  
830 20(1):115.
- 831 Chun, M. and Turk-Browne, N. (2007). Interactions between attention and memory. *Current opinion*  
832 *in neurobiology*, 17(2):177–184.
- 833 Clewett, D. and Davachi, L. (2017). The ebb and flow of experience determines the temporal  
834 structure of memory. *Curr Opin Behav Sci*, 17:186–193.
- 835 Dobrushin, R. L. (1970). Prescribing a system of random variables by conditional distributions.  
836 *Theory of Probability & Its Applications*, 15(3):458–486.
- 837 DuBrow, S. and Davachi, L. (2013). The influence of contextual boundaries on memory for the  
838 sequential order of events. *Journal of Experimental Psychology: General*, 142(4):1277–1286.
- 839 Ezzyat, Y. and Davachi, L. (2011). What constitutes an episode in episodic memory? *Psychological*  
840 *Science*, 22(2):243–252.
- 841 Friendly, M., Franklin, P. E., Hoffman, D., and Rubin, D. C. (1982). The Toronto Word Pool:  
842 Norms for imagery, concreteness, orthographic variables, and grammatical usage for 1,080  
843 words. *Behavior Research Methods and Instrumentation*, 14:375–399.
- 844 Hasson, U., Chen, J., and Honey, C. J. (2015). Hierarchical process memory: memory as an integral  
845 component of information processing. *Trends in Cognitive Science*, 19(6):304–315.
- 846 Hasson, U., Yang, E., Vallines, I., Heeger, D. J., and Rubin, N. (2008). A hierarchy of temporal  
847 receptive windows in human cortex. *Journal of Neuroscience*, 28(10):2539–2550.
- 848 Heusser, A. C., Ezzyat, Y., Shiff, I., and Davachi, L. (2018a). Perceptual boundaries cause mnemonic  
849 trade-offs between local boundary processing and across-trial associative binding. *Journal of*  
850 *Experimental Psychology Learning, Memory, and Cognition*, 44(7):1075–1090.

- 851 Heusser, A. C., Fitzpatrick, P. C., Field, C. E., Ziman, K., and Manning, J. R. (2017). Quail: a  
852 Python toolbox for analyzing and plotting free recall data. *The Journal of Open Source Software*,  
853 10.21105/joss.00424.
- 854 Heusser, A. C., Ziman, K., Owen, L. L. W., and Manning, J. R. (2018b). HyperTools: a Python  
855 toolbox for gaining geometric insights into high-dimensional data. *Journal of Machine Learning  
856 Research*, 18(152):1–6.
- 857 Howard, M. W. and Kahana, M. J. (2002). A distributed representation of temporal context. *Journal  
858 of Mathematical Psychology*, 46:269–299.
- 859 Howard, M. W., MacDonald, C. J., Tiganj, Z., Shankar, K. H., Du, Q., Hasselmo, M. E., and H., E.  
860 (2014). A unified mathematical framework for coding time, space, and sequences in the medial  
861 temporal lobe. *Journal of Neuroscience*, 34(13):4692–4707.
- 862 Howard, M. W., Viskontas, I. V., Shankar, K. H., and Fried, I. (2012). Ensembles of human MTL  
863 neurons “jump back in time” in response to a repeated stimulus. *Hippocampus*, 22:1833–1847.
- 864 Huk, A., Bonnen, K., and He, B. J. (2018). Beyond trial-based paradigms: continuous behavior, on-  
865 going neural activity, and naturalistic stimuli. *Journal of Neuroscience*, 10.1523/JNEUROSCI.1920-  
866 17.2018.
- 867 Kahana, M. J. (1996). Associative retrieval processes in free recall. *Memory & Cognition*, 24:103–109.
- 868 Kelly, S., Lloyd, D., Nurmikko, T., and Roberts, N. (2007). Retrieving autobiographical memories  
869 of painful events activates the anterior cingulate cortex and inferior frontal gyrus. *THe Journal of  
870 Pain*, 8(4):307–314.
- 871 Koriat, A. and Goldsmith, M. (1994). Memory in naturalistic and laboratory contexts: distin-  
872 guishing accuracy-oriented and quantity-oriented approaches to memory assessment. *Journal of  
873 Experimental Psychology: General*, 123(3):297–315.
- 874 Kriegeskorte, N., Mur, M., and Bandettini, P. (2008). Representational similarity analysis – con-  
875 necting the branches of systems neuroscience. *Frontiers in Systems Neuroscience*, 2:1 – 28.

- 876 Landauer, T. K., Foltz, P. W., and Laham, D. (1998). Introduction to latent semantic analysis.
- 877 *Discourse Processes*, 25:259–284.
- 878 Lerner, Y., Honey, C. J., Silbert, L. J., and Hasson, U. (2011). Topographic mapping of a hierarchy  
879 of temporal receptive windows using a narrated story. *Journal of Neuroscience*, 31(8):2906–2915.
- 880 Manning, J. R. (2019). Episodic memory: mental time travel or a quantum ‘memory wave’ function?  
881 *PsyArXiv*, doi:10.31234/osf.io/6zjwb.
- 882 Manning, J. R., Norman, K. A., and Kahana, M. J. (2015). The role of context in episodic memory.  
883 In Gazzaniga, M., editor, *The Cognitive Neurosciences, Fifth edition*, pages 557–566. MIT Press.
- 884 Manning, J. R., Polyn, S. M., Baltuch, G., Litt, B., and Kahana, M. J. (2011). Oscillatory patterns  
885 in temporal lobe reveal context reinstatement during memory search. *Proceedings of the National  
886 Academy of Sciences, USA*, 108(31):12893–12897.
- 887 McInnes, L., Healy, J., and Melville, J. (2018). UMAP: Uniform manifold approximation and  
888 projection for dimension reduction. *arXiv*, 1802(03426).
- 889 Medford, N. and Critchley, H. D. (2010). Conjoint activity of anterior insular and anterior cingulate  
890 cortex: awareness and response. *Brain Structure and Function*, 214(5-6):535–549.
- 891 Menon, V. and Uddin, L. Q. (2010). Saliency, switching, attention and control: a network model of  
892 insula function. *Brain Structure and Function*, 214(5-6):655–667.
- 893 Mikolov, T., Chen, K., Corrado, G., and Dean, J. (2013). Efficient estimation of word representations  
894 in vector space. *arXiv*, 1301.3781.
- 895 Mueller, A., Fillion-Robin, J.-C., Boidol, R., Tian, F., Nechifor, P., yoonsubKim, Peter, Rampin, R.,  
896 Corvellec, M., Medina, J., Dai, Y., Petrushev, B., Langner, K. M., Hong, Alessio, Ozsvald, I.,  
897 vkolmakov, Jones, T., Bailey, E., Rho, V., IgorAPM, Roy, D., May, C., foobuzz, Piyush, Seong,  
898 L. K., Goey, J. V., Smith, J. S., Gus, and Mai, F. (2018). WordCloud 1.5.0: a little word cloud  
899 generator in Python. *Zenodo*, <https://zenodo.org/record/1322068#.W4tPKZNKh24>.

- 900 Murdock, B. B. (1962). The serial position effect of free recall. *Journal of Experimental Psychology*,  
901 64:482–488.
- 902 Paller, K. A. and Wagner, A. D. (2002). Observing the transformation of experience into memory.  
903 *Trends in Cognitive Sciences*, 6(2):93–102.
- 904 Pedregosa, F., Varoquaux, G., Gramfort, A., Michel, V., Thirion, B., Grisel, O., Blondel, M., Pretten-  
905 hofer, P., Weiss, R., Dubourg, V., Vanderplas, J., Passos, A., Cournapeau, D., Brucher, M., Perrot,  
906 M., and Duchesnay, E. (2011). Scikit-learn: Machine learning in Python. *Journal of Machine  
907 Learning Research*, 12:2825–2830.
- 908 Polyn, S. M., Norman, K. A., and Kahana, M. J. (2009). A context maintenance and retrieval model  
909 of organizational processes in free recall. *Psychological Review*, 116(1):129–156.
- 910 Postman, L. and Phillips, L. W. (1965). Short-term temporal changes in free recall. *Quarterly Journal  
911 of Experimental Psychology*, 17:132–138.
- 912 Rabiner, L. (1989). A tutorial on Hidden Markov Models and selected applications in speech  
913 recognition. *Proceedings of the IEEE*, 77(2):257–286.
- 914 Radvansky, G. A. and Zacks, J. M. (2017). Event boundaries in memory and cognition. *Curr Opin  
915 Behav Sci*, 17:133–140.
- 916 Ramdas, A., Trillos, N., and Cuturi, M. (2017). On wasserstein two-sample testing and related  
917 families of nonparametric tests. *Entropy*, 19(2):47.
- 918 Ranganath, C. and Ritchey, M. (2012). Two cortical systems for memory-guided behavior. *Nature  
919 Reviews Neuroscience*, 13:713 – 726.
- 920 Simony, E., Honey, C. J., Chen, J., and Hasson, U. (2016). Uncovering stimulus-locked network  
921 dynamics during narrative comprehension. *Nature Communications*, 7(12141):1–13.
- 922 Stark, S. M., Yassa, M. A., and Stark, C. E. L. (2010). Individual differences in spatial pattern  
923 separation performance associated with healthy aging in humans. *Learning & Memory*, 17(6):284–  
924 288.

- 925 Steyvers, M., Shiffrin, R. M., and Nelson, D. L. (2004). Word association spaces for predicting  
926 semantic similarity effects in episodic memory. In Healy, A. F., editor, *Cognitive Psychology and*  
927 *its Applications: Festschrift in Honor of Lyle Bourne, Walter Kintsch, and Thomas Landauer*. American  
928 Psychological Association, Washington, DC.
- 929 Tomrary, A. and Davachi, L. (2017). Consolidation promotes the emergence of representational  
930 overlap in the hippocampus and medial prefrontal cortex. *Neuron*, 96(1):228–241.
- 931 Tyng, C. M., Amin, H. U., Saad, M. N. M., and S, M. A. (2017). The influences of emotion on  
932 learning and memory. *Frontiers in psychology*, 8:1454.
- 933 Waskom, M., Botvinnik, O., Okane, D., Hobson, P., David, Halchenko, Y., Lukauskas, S., Cole, J. B.,  
934 Warmenhoven, J., de Ruiter, J., Hoyer, S., Vanderplas, J., Villalba, S., Kunter, G., Quintero, E.,  
935 Martin, M., Miles, A., Meyer, K., Augspurger, T., Yarkoni, T., Bachant, P., Williams, M., Evans,  
936 C., Fitzgerald, C., Brian, Wehner, D., Hitz, G., Ziegler, E., Qalieh, A., and Lee, A. (2016). Seaborn:  
937 v0.7.1.
- 938 Welch, G. B. and Burnett, C. T. (1924). Is primacy a factor in association-formation. *American Journal*  
939 *of Psychology*, 35:396–401.
- 940 Yarkoni, T., Poldrack, R. A., Nichols, T. E., Van Essen, D. C., and Wager, T. D. (2011). Large-scale  
941 automated synthesis of human functional neuroimaging data. *Nature Methods*, 8(8):665.
- 942 Yassa, M. A., Lacy, J. W., Stark, S. M., Albert, M. S., Gallagher, M., and Stark, C. E. L. (2011). Pattern  
943 separation deficits associated with increased hippocampal ca3 and dentate gyrus activity in  
944 nondemented older adults. *Hippocampus*, 21(9):968–979.
- 945 Yassa, M. A. and Stark, C. E. L. (2011). Pattern separation in the hippocampus. *Trends In Neuro-*  
946 *sciences*, 34(10):515–525.
- 947 Yonelinas, A. P. (2002). The nature of recollection and familiarity: A review of 30 years of research.  
948 *Journal of Memory and Language*, 46:441–517.

- 949 Yonelinas, A. P., Kroll, N. E., Quamme, J. R., Lazzara, M. M., Sauvé, M. J., Widaman, K. F., and  
950 Knight, R. T. (2002). Effects of extensive temporal lobe damage or mild hypoxia on recollection  
951 and familiarity. *Nature Neuroscience*, 5(11):1236–41.
- 952 Zacks, J. M., Speer, N. K., Swallow, K. M., Braver, T. S., and Reynolds, J. R. (2007). Event perception:  
953 a mind-brain perspective. *Psychological Bulletin*, 133:273–293.
- 954 Zadbood, A., Chen, J., Leong, Y. C., Norman, K. A., and Hasson, U. (2017). How we transmit  
955 memories to other brains: Constructing shared neural representations via communication. *Cereb  
956 Cortex*, 27(10):4988–5000.
- 957 Zwaan, R. A. and Radvansky, G. A. (1998). Situation models in language comprehension and  
958 memory. *Psychological Bulletin*, 123(2):162 – 185.

## 959 **Supporting information**

960 Supporting information is available in the online version of the paper.

## 961 **Acknowledgements**

962 We thank Luke Chang, Janice Chen, Chris Honey, Lucy Owen, Emily Whitaker, and Kirsten Ziman  
963 for feedback and scientific discussions. We also thank Janice Chen, Yuan Chang Leong, Kenneth  
964 Norman, and Uri Hasson for sharing the data used in our study. Our work was supported in part  
965 by NSF EPSCoR Award Number 1632738. The content is solely the responsibility of the authors  
966 and does not necessarily represent the official views of our supporting organizations.

## 967 **Author contributions**

968 Conceptualization: A.C.H. and J.R.M.; Methodology: A.C.H., P.C.F. and J.R.M.; Software: A.C.H.,  
969 P.C.F. and J.R.M.; Analysis: A.C.H., P.C.F. and J.R.M.; Writing, Reviewing, and Editing: A.C.H.,

<sup>970</sup> P.C.F. and J.R.M.; Supervision: J.R.M.

<sup>971</sup> **Author information**

<sup>972</sup> The authors declare no competing financial interests. Correspondence and requests for materials  
<sup>973</sup> should be addressed to J.R.M. (jeremy.r.manning@dartmouth.edu).